DOI: 10.1002/chem.200601884

Synthetic Models of the Active Site of Cytochrome *c* Oxidase: Influence of Tridentate or Tetradentate Copper Chelates Bearing a His–Tyr Linkage Mimic on Dioxygen Adduct Formation by Heme/Cu Complexes

Jin-Gang Liu, Yoshinori Naruta,* and Fumito Tani[a]

Abstract: Two synthetic models of the active site of cytochrome *c* oxidase—$[(L^{N4\text{-}OH})Cu^{I}\text{-}Fe^{II}(TMP)]^{+}$ (**1a**) and $[(L^{N3\text{-}OH})Cu^{I}\text{-}Fe^{II}(TMP)]^{+}$ (**2a**)—have been designed and synthesized. These models each contain a heme and a covalently attached copper moiety supported either by a tetradentate N4-copper chelate or by a tridentate N3-copper chelate including a moiety that acts as a mimic of the crosslinked His-Tyr component of cytochrome *c* oxidase. Low-temperature oxygenation reactions of these models have been investigated by spectroscopic methods including UV/Vis, resonance Raman, ESI-MS, and EPR spectroscopy. Oxygenation of the tetradentate model **1a** in MeCN and in other solvents produces a low-temperature-stable dioxygen-bridged peroxide $[(L^{N4\text{-}OH})Cu^{II}\text{-}O_2\text{-}Fe^{III}\text{-}(TMP)]^{+}$ $\{\nu_{O\text{-}O} = 799\ (^{16}O_2)/752\ cm^{-1}\ (^{18}O_2)\}$, while a heme superoxide species $[(TMP)Fe^{III}(O_2^{-})\cdots Cu^{II}L^{N3\text{-}OH}]$ $\{\nu_{Fe\text{-}O_2}$: 576 $(^{16}O_2)/551\ cm^{-1}$ $(^{18}O_2)\}$ is generated when the tridentate model **2a** is oxygenated in EtCN solution under similar experimental conditions. The coexistence of a heme superoxide species $[(TMP)Fe^{III}(O_2^{-})\cdots Cu^{II}L^{N3\text{-}OH}]$ and a bridged peroxide $[(L^{N3\text{-}OH})Cu^{II}\text{-}O_2\text{-}Fe^{III}(TMP)]^{+}$ species in equal amounts is observed when the oxygenation reaction of **2a** is performed in CH_2Cl_2/7% EtCN, while the percentage of the peroxide (≈70%) in relation to superoxide (≈30%) increases further when the crosslinked phenol moiety in **2a** is deprotonated to produce the bridged peroxide $[(L^{N3\text{-}OH})Cu^{II}\text{-}O_2\text{-}Fe^{III}(TMP)]^{+}$ $\{\nu_{O\text{-}O}$: 812 $(^{16}O_2)/765\ cm^{-1}$ $(^{18}O_2)\}$ as the main dioxygen intermediate. The weak reducibility and decreased O_2 reactivity of the tricoordinated Cu^{I} site in **2a** are responsible for the solvent-dependent formation of dioxygen adducts. The initial binding of dioxygen to the copper site en route to the formation of a bridged heme-O_2-Cu intermediate by model **2a** is suggested and the deprotonated crosslinked His-Tyr moiety might contribute to enhancement of the O_2 affinity of the Cu^{I} site at an early stage of the dioxygen-binding process.

Keywords: copper complex · cytochrome *c* oxidase · dioxygen activation · enzyme models · heme proteins

Introduction

Cytochrome *c* oxidase (C*c*O), the terminal enzyme in the respiratory chain, catalyzes the thermodynamically favorable four-electron reduction of dioxygen to water and concomitantly pumps four protons across the mitochondrial or bacterial membrane, generating the electrochemical proton gradient used by ATP synthase for the formation of ATP.[1] The reduction of dioxygen to water takes place at the heme a_3-Cu_B binuclear center, with an iron–copper separation of about 5.0 Å. Cu_B is coordinated by three histidine residues. The current consensus with regard to the process of O_2-binding and reduction during the C*c*O catalytic cycle is that the process occurs through an initial association of dioxygen with Cu_B, followed by transfer of O_2 to heme a_3, to form the first spectroscopically observable intermediate: compound **A** (Fe^{III}-superoxo). The next detectable intermediate has already undergone O–O bond cleavage to produce the ferryl-oxo (Fe^{IV}=O) species (compound **P**) and Cu_B^{II}–OH. The heterolytic O–O bond cleaving process and other details remain to be clarified. A bridging peroxo species (Fe^{III}-O-O-Cu^{II}) has been proposed as a possible intermediate in the catalytic cycle,[2] but has yet to be observed during the course of the enzymatic reaction. Since X-ray crystallographic analysis revealed an unprecedented crosslink between one of the Cu_B-coordinated histidine ligands

[a] Dr. J.-G. Liu, Prof. Dr. Y. Naruta, Dr. F. Tani
Institute for Materials Chemistry and Engineering
Kyushu University, Higashi-ku, Fukuoka, 812-8581 (Japan)
Fax: (+81) 92-642-2731
E-mail: naruta@ms.ifoc.kyushu-u.ac.jp

Supporting information for this article is available on the WWW under http://www.chemeurj.org/ or from the author.

and a tyrosine residue (Figure 1),[3] intense efforts to elucidate the role(s) of this novel His-Tyr crosslink during the catalytic cycle of O_2 reduction have been undertaken. Al-

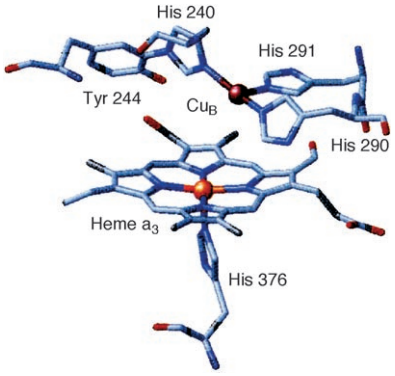

Figure 1. Dioxygen metabolic site structure of bovine heart cytochrome *c* oxidase.[3b]

though several functional/structural roles for the crosslinked His-Tyr-Cu$_B$ moiety have been proposed, its exact role remains elusive.[4] Recent investigations suggest that the processes of binding and fission of dioxygen are responsible for driving internal proton rearrangements, such as deprotonation of the crosslinked tyrosine.[5]

The not fully understood mechanism of dioxygen reduction by C*c*O has inspired many chemists to model aspects of its active binding site and related chemical properties. Numerous heme/copper systems designed as synthetic functional models have been reported and investigations of their reactions with O_2 have provided fundamental insights into the reactivity of the enigmatic heme a_3/Cu$_B$ binuclear center in C*c*O.[6] However, the majority of the reported biomimetic models lack a crosslinked His-Tyr mimic moiety, which appears to play important roles in the process of C*c*O-catalyzed dioxygen reduction. Examples of binucleating ligands bearing a Tyr mimic and synthetic analogues of the His-Tyr crosslinkage and their Cu and Zn complexes have recently been reported,[7–9] but O_2 reaction studies that combine a Cu$_B$ site mimic with a heme component are still very rare. Karlin and co-workers reported an oxygenation reaction of an untethered heme/copper assembly in which a crosslinked imidazole–phenol was employed as a part of the tetradentate copper ligand.[10] In our preliminary communication, we reported the first example of a covalently appended tetradentate copper ligand incorporating a crosslinked imidazole–phenol derivative with a heme functional group (Figure 2, **1a**).[11] The resultant heme/copper compound reacts with dioxygen to form a peroxide species that is stable at low temperature. In a very recent paper[12] we described a fully integrated C*c*O model ($L^{N4\text{-}OH}Cu^{I}$-Fe^{II}TMPIm) possessing a His-Tyr crosslink mimic and a heme a_3 axial imidazole ligand. This model complex undergoes a unique transformation from a heme-μ-peroxo-Cu^{II} species to a heme-superoxo/Cu^{I} intermediate in the course of the oxygenation reaction at low temperature.

To refine our model of the C*c*O tridentate $(His)_2Cu_B(His\text{-}Tyr)$ site further and to obtain further insights into the dioxygen reduction mechanism, we prepared $[(L^{N3\text{-}OH})Cu^{I}\text{-}Fe^{II}\text{-}(TMP)]^+$ (**2a**, Figure 2), which represents a new example of

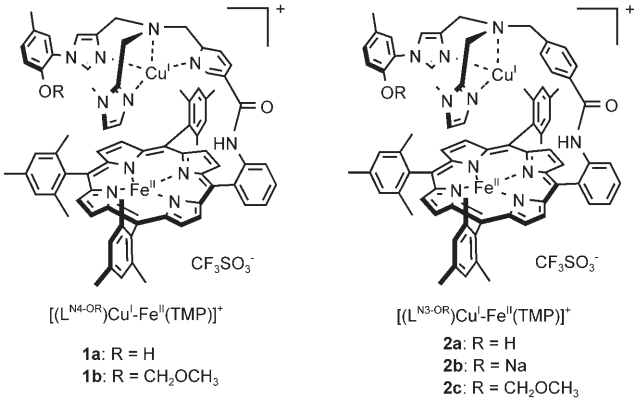

Figure 2. Chemical structures of the model compounds.

a covalently tethered heme/Cu C*c*O model bearing a tridentate N3-copper chelate with a moiety acting as a crosslinked His-Tyr mimic. The oxygenation reaction of the N3-copper chelate heme/copper model compound produces a heme superoxide intermediate in nitrile solvents, while in CH_2Cl_2/7% EtCN the coexistence of a heme superoxide and a bridged heme-O_2-Cu peroxide species in equivalent amounts is observed. Additionally, deprotonation of the crosslinked phenol moiety results in an increased ratio of peroxide to superoxide. The process of solvent-dependent formation of dioxygen adducts by model **2a** differs from that of its tetradentate counterpart **1a** ($[(L^{N4\text{-}OH})Cu^{I}\text{-}Fe^{II}(TMP)]^+$; Figure 2), which only forms a bridged peroxide in a variety of solvents. In this report we describe the details of the syntheses of these model compounds and the formation of the corresponding low-temperature dioxygen adducts in different solvents as observed by UV/Vis, resonance Raman, ESI-MS, and EPR spectroscopy.

Results and Discussion

Design and syntheses: The copper complex $[Cu(OH)TMEDA]_2Cl_2$ (TMEDA = *N*,*N*,*N*′,*N*′-tetramethylethylenediamine), previously developed for C–C bond oxidative homocoupling of naphthols or alkynes,[13] had been reported to catalyze the formation of C–N bonds between commercially available arylboronic acids and imidazole derivatives efficiently at room temperature.[14] This system has the advantage of employing mild, abasic conditions, but it has only been applied for a limited number of substrates. When performed on a 4-substituted imidazole, the reaction has afforded mixtures of regioisomers that have not been isolated. Here we extend this approach to the preparation of *N*-arylimidazoles as building

blocks of new model compounds, incorporating the *N*-(2′-hydroxyphenyl)imidazole moiety as the Cu_B site mimic.

Scheme 1 shows the preparation of the tripodal copper moiety for the model compounds. The methoxymethyl-protected (MOM-protected) 2-hydroxyphenylboronic acid **3** was prepared in 65% overall yield by sequential reactions involving metallation (*n*BuLi/Et_2O/−70°C) of MOM-protected 2-bromo-4-methylphenol and treatment with $B(OMe)_3$, followed by acidic workup. Compound **4**, in which the hydroxy group is protected by a *tert*-butyldiphenylsilyl group (TBDPS), was readily prepared in a high yield of 92% from 4-(hydroxymethyl)imidazole hydrochloride by treatment with *tert*-butyl(chloro)diphenylsilane and imidazole in DMF. The preparation of **5a** was performed by coupling of **3** (1.1 equiv) with 4-(*tert*-butyldiphenylsilanyloxymethyl)-1*H*-imidazole (**4**, 1.0 equiv) in the presence of $[Cu(OH)TMEDA]_2Cl_2$ (10 mol%) and oxygen in CH_2Cl_2 at room temperature over 48 h. The resulting two isomers **5a** and **5b** were readily separable by silica gel column chromatography in yields of 75 and 7%, respectively; the regioselectivity of this reaction is about 10:1. It is noteworthy that when 1*H*-imidazole-4-carbaldehyde was employed in the coupling reaction, none of the desired product was obtained, while a change in the protecting group in **4** from TBDPS (*t*$BuPh_2Si$) to TBDMS (*t*$BuMe_2Si$) decreased both the reaction yield (57%) and the regioselectivity (3:1). The steric hindrance and introduction of a substituent at the 4-position in imidazole appear to have a remarkable effect on yield and regioselectivity. Since *ortho*-methoxyphenylboronic acids have been found to depress cross-coupling yields severely,[14] we chose MOM to protect the phenolic hydroxy group. This choice of protecting group was also based on the following requirements: 1) it should tolerate basic or mildly acidic conditions during further reaction steps; 2) it should be compact enough to avoid possible steric hindrance during the *N*-arylation of imidazoles, and 3) it should be removable under mild conditions at the final step.

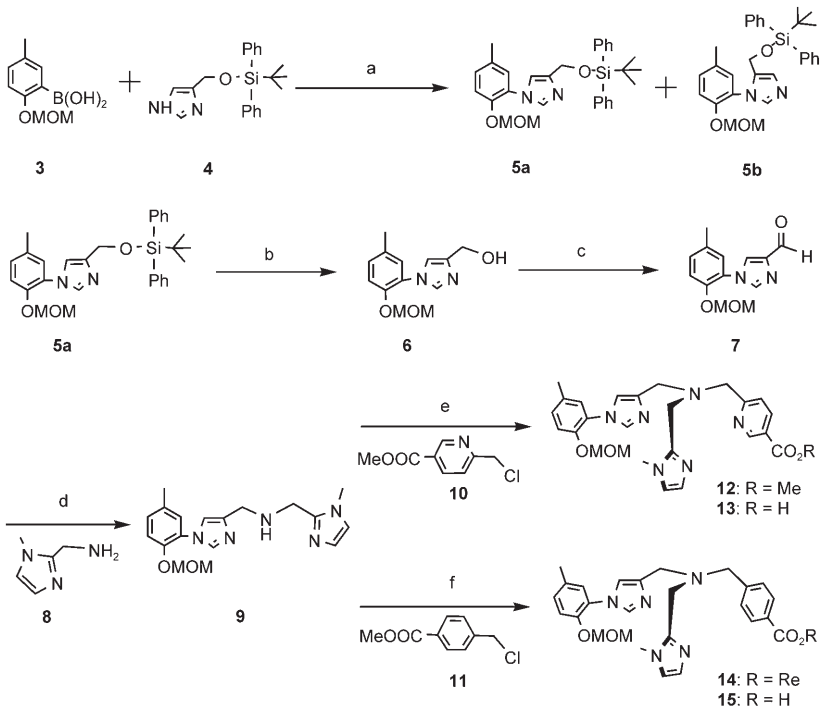

Scheme 1. Preparation of the tripodal copper ligand for the model compounds. a) cat. $[Cu(OH)TMEDA]_2Cl_2$, CH_2Cl_2, O_2, RT, 75%; b) *n*BuN^+F^-, THF, RT, 93%; c) MnO_2, $CHCl_3$, reflux, 85%; d) 1) Et_3N, MeOH, 2) $NaBH_4$, 65%; e) 1) K_2CO_3, CH_3CN, RT, 61%, 2) KOH, THF, RT, 86%; f) 1) Et_3N, CH_3CN, RT, 45%, 2) KOH, THF, RT, 90%.

The isolated *N*-arylimidazole **5a** was converted into **7** by sequential deprotection of compound **5a** in THF and oxidation with freshly prepared MnO_2 in chloroform. Treatment of **7** with 2-aminomethylimidazole (**8**) in methanol generated the corresponding Schiff base intermediate, which was subsequently reduced in situ with $NaBH_4$ to give **9** in a yield of 65%. The tripodal ligands **13** and **15** were obtained as follows: the amine **9** was first treated with methyl 6-(chloromethyl)nicotinate (**10**) or methyl *m*-(chloromethyl)benzoate (**11**) in the presence of a base such as K_2CO_3 or Et_3N in CH_3CN, and the resultant products were then hydrolyzed in KOH solution to provide moderate overall yields. The tripodal ligands thus prepared are important building blocks used in the assembly of C*c*O active site models.

The syntheses of the binucleating ligands **17** (Scheme 2) and **19** (Scheme 3) were completed in subsequent steps. The condensation reactions between **13** or **15** and the porphyrin **16** ($TMPNH_2$: 2-[10,15,20-tris(2,4,6-trimethylphenyl)porphyrin-5-yl]phenylamine) were performed in the presence of Et_3N/2-(chloromethyl)pyridium iodide in CH_2Cl_2 to give the covalent conjugates **17** (63%) and **19** (45%), respectively. The MOM group in **17** was removed with bromotrimethylsilane in CH_2Cl_2 at −30°C to produce the binucleating free hydroxy ligand **18** ($L^{N4\text{-}OH}TMP$) in a moderate yield of 60% (Scheme 2), and addition of an excess of $FeBr_2$ to the porphyrin **18** in THF at reflux, followed by extraction with degassed aqueous Na_2EDTA solution, produced the corresponding mononuclear Fe^{II} porphyrin. Further addition of one equivalent of copper salt $[Cu(CH_3CN)_4]^+$ (TfO^-) provided the desired model compound **1a**.

Compound **2a** was prepared through a similar stepwise metallation reaction with a minor alteration (Scheme 3): the removal of the MOM group was carried out after insertion

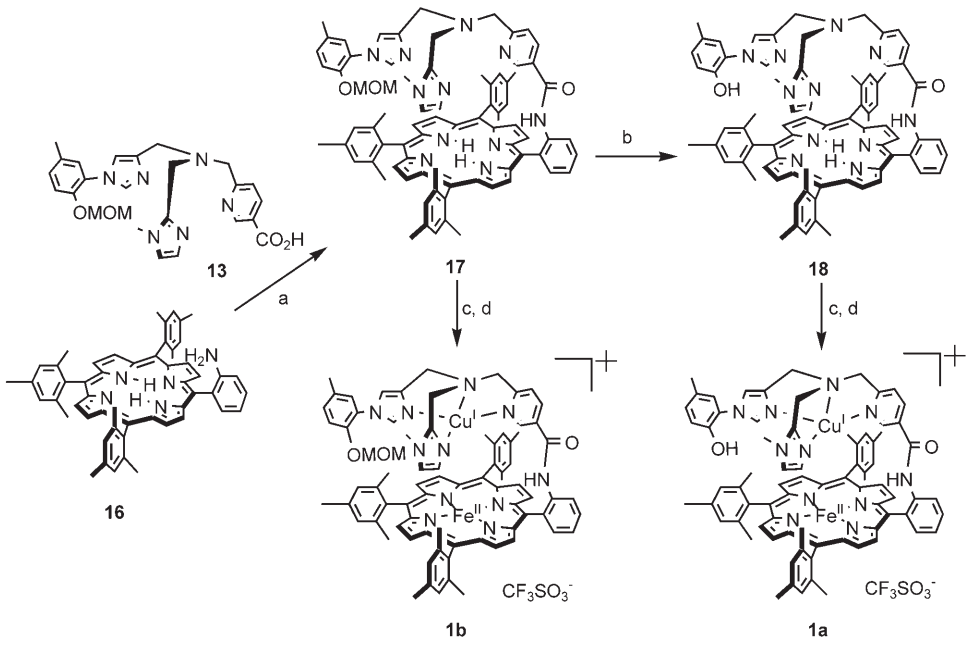

Scheme 2. a) 2-(Chloromethyl)pyridinium iodide, Et_3N, CH_2Cl_2, RT, 63%; b) Me_3SiBr, CH_2Cl_2, −30°C, 60%; c) $FeBr_2$, THF, Na_2EDTA; d) $[Cu^I(CH_3CN)_4]\cdot(CF_3SO_3)$, RT, 94% (**1a**), 95% (**1b**).

of iron into the porphyrin. This alteration raises the yield to 80%. Compound **2b**, containing the deprotonated cross-linked imidazole–phenol moiety, was prepared by treatment of the dithionite reduced THF solution of compound **21** with a degassed aqueous Na_2CO_3 solution.

Oxygenation of $[(L^{N4\text{-}OH})Cu^I\text{-}Fe^{II}(TMP)]^+$ (1a): Oxygenation of **1a** in MeCN at −30°C resulted in significant UV/Vis spectroscopic changes (Figure S1, Supporting Information). The reduced form has absorption maxima at 429 nm (ε = 82500 $M^{-1}cm^{-1}$), 533 nm (ε = 9700 $M^{-1}cm^{-1}$), and 569 nm (ε = 4000 $M^{-1}cm^{-1}$), and the introduction of O_2 produces a stable dioxygen adduct with new spectral features at 421 nm (ε = 57000 $M^{-1}cm^{-1}$), 558 nm (ε = 8000 $M^{-1}cm^{-1}$) and 614 nm (ε = 3800 $M^{-1}cm^{-1}$). The UV/Vis spectrum of the dioxygen adduct resembles that of the dioxygen-bridged heme-peroxo-copper complex [(5Me-TPA)Cu^{II}-O_2-Fe^{III}(TMP)]$^+$, which has absorption maxima at 420 nm, 557 nm, and 612 nm in MeCN and the structure of which has been determined by X-ray crystallographic analysis.[15] Application of a vacuum does not affect the UV/Vis features of the oxy form, which indicates that the formation of the dioxygen adduct is irreversible and stable at −30°C. The dioxygen adduct is also stable in solvent mixtures such as MeCN/THF and MeCN/CH_2Cl_2, but its thermal stability decreases in CH_2Cl_2 and toluene.

A dioxygen adduct is also generated on oxygenation of the MOM-protected model **1b**

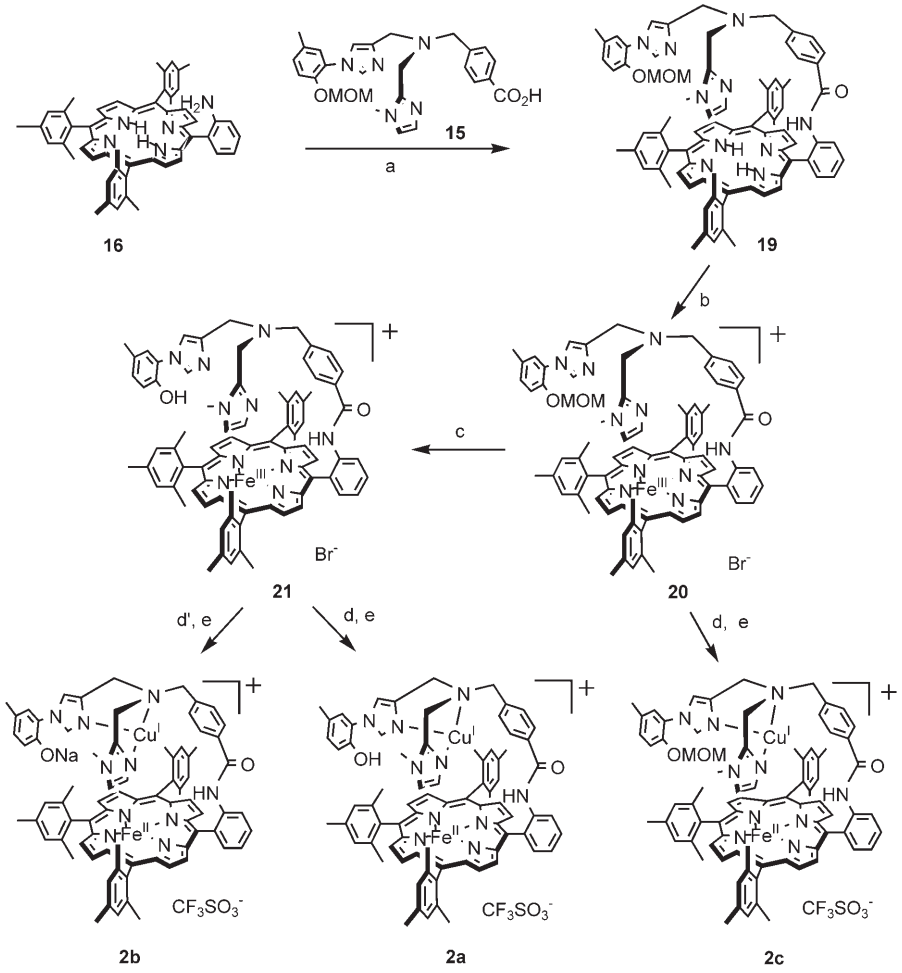

Scheme 3. a) 2-(Chloromethyl)pyridinium iodide, Et_3N, CH_2Cl_2, RT, 45%; b) $FeBr_2$, THF, Na_2EDTA, 88%; c) Me_3SiBr, CH_2Cl_2, −30°C, 80%; d) $Na_2S_2O_4$, THF/toluene, RT; d′) $Na_2S_2O_4$, THF/toluene, 0.1 M Na_2CO_3 (aq.), RT; e) $[Cu^I(CH_3CN)_4]\cdot(CF_3SO_3)$, RT, 94% (**2a**), 93% (**2b**), 95% (**2c**).

in MeCN, exhibiting UV/Vis features and thermal stability similar to those of **1a** (Figure S2, Supporting Information).

Resonance Raman (rR) spectroscopy was used to characterize the dioxygen adduct under the same experimental conditions as used for UV/Vis spectroscopic measurements. The rR spectrum of the dioxygen adduct of **1a** measured in MeCN at −30 °C indicates that it is a peroxo complex with a high-spin ferric heme configuration. In the high-frequency region of the rR spectrum, the spin-state maker band (ν_2) appears at 1552 cm^{-1}, while the peak at 1359 cm^{-1} is attributable to the oxidation-state maker band (ν_4) of the porphyrin. An oxygen isotope-sensitive band at 799 cm^{-1} that shifts by −47 cm^{-1} with $^{18}O_2$ substitution is observed in the low-frequency region (Figure S3, Supporting Information).

Table 1. Resonance Raman data for heme-peroxo-copper complexes.

Complexes	ν_{O-O} $\nu(^{16}O_2)/\nu(^{18}O_2)$	References
tetradentate N4-copper chelate		
$[(L^{N4\text{-}OH})Cu^{II}\text{-}O_2\text{-}Fe^{III}(TMP)]^+$ (**1a**)	799/752	this work
$[(L^{N4\text{-}OMOM})Cu^{II}\text{-}O_2\text{-}Fe^{III}(TMP)]^+$ (**1b**)	801/755	this work
$[(5MeTPA)Cu^{II}\text{-}O_2\text{-}Fe^{III}(TMP)]^+$	790/746	[15]
$[(TPA)Cu^{II}\text{-}O_2\text{-}Fe^{III}(TPP)]^+$	803/759	[16c]
$[(5MeTPA)Cu^{II}\text{-}O_2\text{-}Fe^{III}(TPP)]^+$	793/751	[16d]
$[(^6L)Cu^{II}\text{-}O_2\text{-}Fe^{III}]^+$	788/744	[16b]
$[(TMPA)Cu^{II}\text{-}O_2\text{-}Fe^{III}(F_8TPP)]^+$	808/762	[16a]
$[(L^{N4}OMe)Cu^{II}\text{-}O_2\text{-}Fe^{III}(F_8TPP)]^+$	815/769	[10]
$[(L^{N4}OH)Cu^{II}\text{-}O_2\text{-}Fe^{III}(F_8TPP)]^+$	813/769	[10]
$[(L^{N4\text{-}OH})Cu^{II}\text{-}O_2\text{-}Fe^{III}(TMPIm)]^+$	803, 787/752	[12]
$[(L^{N4\text{-}OMOM})Cu^{II}\text{-}O_2\text{-}Fe^{III}(TMPIm)]^+$	804, 788/752	[12]
tridentate N3-copper chelate		
$(L^{N3\text{-}OH})Cu^{II}\text{-}O_2\text{-}Fe^{III}(TMP)]^+$ (**2a**)	810/764	this work
$[(L^{N4\text{-}ONa})Cu^{II}\text{-}O_2\text{-}Fe^{III}(TMP)]^+$ (**2b**)	812/765	this work
$[(^2L)Cu^{II}\text{-}O_2\text{-}Fe^{III}]^+$	747/707	[21a]
$[(L^{Me2N})Cu^{II}\text{-}O_2\text{-}Fe^{III}(F_8TPP)]^+$	767/726, 752/707	[21b]
$[(DHIm)(TACN)Cu^{II}\text{-}O_2\text{-}Fe^{III}]^+$	758/740	[21c]

ESI mass spectrometry is very useful for the study and characterization of the relatively stable peroxides described here. The mass spectrum of the reduced form **1a** exhibits a parent ion at 1286.5 ($[M-TfO]^+$)—1330.5 ($[M-TfO]^+$) for **1b**—and this shifts to peaks centered at 1318.5 ($[M-TfO]^+$)—1362.5 ($[M-TfO]^+$) for **1b**—when $^{16}O_2$ is introduced to the solution. The observed isotope distribution of peaks agrees very well with the simulated pattern based on the ratio of Fe^{II}-Cu^{I}/O_2 1:1 (Figure 3 and Figure S5, Supporting Information). The expected increase of 4 amu is observed when $^{18}O_2$ is substituted. Frozen solutions (CH_3CN, 77 K) of the dioxygen adducts of **1a** and **1b** are EPR silent, which indicates the occurrence of antiferromagnetic coupling between the two paramagnetic metals and provides further evidence of formation of a dioxygen-bridged peroxide.

From evidence obtained from UV/Vis, rR, ESI mass, and EPR experiments, we conclude that the oxygenation reactions of the tetradentate N4-copper chelate heme/Cu models (**1a** and **1b**) in MeCN generate dioxygen-bridged peroxo complexes $[(L^{N4\text{-}OR})Cu^{II}\text{-}O_2\text{-}Fe^{III}(TMP)]^+$ (**1a**: R = H; **1b**: R = MOM). Given the similarities of the spectroscopic properties to those of $[(5MeTPA)Cu^{II}\text{-}O_2\text{-}Fe^{III}(TMP)]^+$, which adopts a $\mu\text{-}\eta^2\text{:}\eta^1$ dioxygen binding mode (η^2 to Fe and η^1 to Cu), we infer that the same dioxygen binding mode exists for the peroxo complexes $[(L^{N4\text{-}OR})Cu^{II}\text{-}O_2\text{-}Fe^{III}(TMP)]^+$ (**1a**: R = H; **1b**: R = MOM) described here.

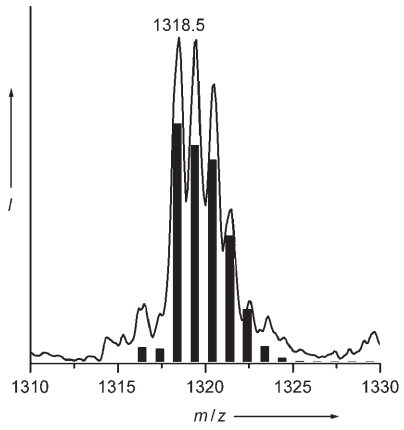

Figure 3. ESI-MS spectrum of $[(L^{N4\text{-}OH})Cu^{II}\text{-}O_2\text{-}Fe^{III}(TMP)]^+$. The solid line shows the observed spectrum and the bars represent the simulated isotope distribution.

Oxygenation of $[(L^{N3\text{-}OH})Cu^{I}\text{-}Fe^{II}(TMP)]^+$ (2a): The UV/Vis spectroscopic changes that occur during the oxygenation reaction of **2a** in propionitrile at −80 °C are shown in Figure 4. Exposure of **2a** to dioxygen gives rise to distinctive spectral changes in the Soret band, with shifting from 427 nm ($\varepsilon = 72\,000\ M^{-1}cm^{-1}$) to 414 nm ($\varepsilon = 56\,800\ M^{-1}cm^{-1}$) and the appearance of a shoulder at 400 nm, while the Q-band at 531 nm becomes flat ($\varepsilon = 8900$ to $4000\ M^{-1}cm^{-1}$). RR spectroscopic investigation of this oxygenation reaction under the same experimental conditions indicates a lack of the characteristic oxygen isotope-sensitive band in the region near 800 cm^{-1} or above. However, an oxygen iso-

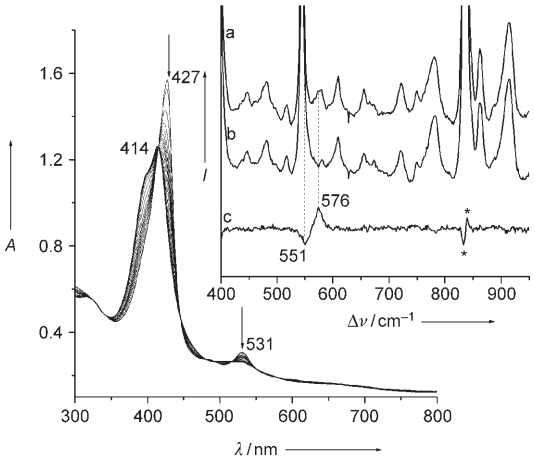

Figure 4. UV/visible spectra changes of **2a** upon oxygenation in EtCN at −80 °C. Inset: Resonance Raman spectra of oxy-**2a** formed from $^{16}O_2$ (a) and $^{18}O_2$ (b). c) Difference spectrum [a) minus b)]. Conditions: EtCN, −80 °C, excitation at 413 nm, 25 mW; * solvent.

tope-sensitive band is observed at 576 ($^{16}O_2$)/551 cm^{-1} ($^{18}O_2$) (Figure 4, inset) with a ν_4 band appearing at 1366 cm^{-1}. The observed isotopic frequency shift [Δ_{obsd}($^{16}O_2$/$^{18}O_2$) = 25 cm^{-1}] matches well with the expected value for the ν_{Fe-O_2} mode in the diatomic harmonic approximation. The reported C*c*O model compound PorFe−O_2/[Cu(NMePr)]$^+$ (570 cm^{-1}),[17] oxymyoglobin (570 cm^{-1}),[18] oxy-C*c*O (572 cm^{-1}),[19] and other well characterized examples of heme superoxide complexes manifest similar Fe−O_2 [ν_{Fe-O_2}] stretching vibrations,[20] so the Raman band at 576 cm^{-1} is assigned to the Fe−O_2 stretching mode of a heme superoxide species. The frozen sample of this dioxygen adduct displays a copper(II) EPR signal of a shape and intensity similar to that of the oxidized form at room temperature (Figure 5c), which suggests that during the course of the oxygenation reaction at −80 °C the copper(I) site is directly oxidized to copper(II). Consequently, the oxygenation reaction of compound **2a** in a nitrile solution results in the formation of a heme superoxide adduct, in contrast to the formation of a dioxygen-bridged peroxide [799 ($^{16}O_2$)/752 cm^{-1} ($^{18}O_2$)] observed with the tetradentate counterpart **1a** in acetonitrile solution as described above.

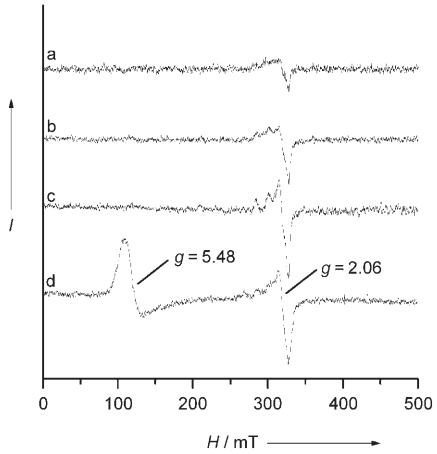

Figure 5. ESR spectra of frozen samples (77 K) of a) oxy-**2b**, and b) oxy-**2a** generated in CH_2Cl_2/7% EtCN at −100 °C. c) Oxy-**2a** generated in EtCN at −80 °C. d) Oxy-**2a** at RT.

When the oxygenation reaction of compound **2a** is carried out in CH_2Cl_2/7% EtCN at −100 °C, it gives rise to electronic absorption spectral changes, with the Soret band shifting from 428 nm (ε = 85 000 M^{-1}cm^{-1}) to 419 nm (ε = 73 000 M^{-1}cm^{-1}) and the Q-band shifting from 532 nm (ε = 7500 M^{-1}cm^{-1}) to 543 nm (ε = 6300 M^{-1}cm^{-1}) (Figure 6). The

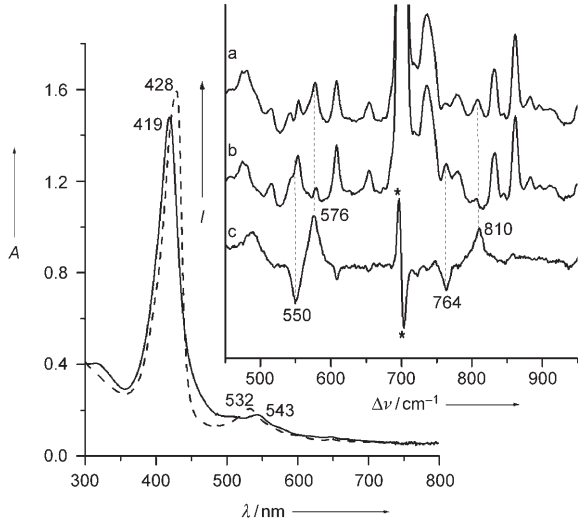

Figure 6. UV/visible spectra of the reduced form (dashed) and the oxy form (solid) of **2a** in CH_2Cl_2/7% EtCN solution at −100 °C. Inset: Resonance Raman spectra of oxy-**2a** formed from $^{16}O_2$ (a) and $^{18}O_2$ (b). c) Difference spectra [a) minus b)]. Conditions: CH_2Cl_2/7% EtCN, −100 °C, excitation at 413 nm, 25 mW; * solvent.

rR spectrum of this oxy form exhibits two groups of isotope-sensitive bands: one at 810 cm^{-1} ($^{16}O_2$)/764 cm^{-1} ($^{18}O_2$), and the other at 576 cm^{-1} ($^{16}O_2$)/550 cm^{-1} ($^{18}O_2$) (Figure 6, inset). The 810 cm^{-1} band is attributable to the O−O stretching [ν_{O_2}] mode, and its value is similar to those in the reported dioxygen adducts in the peroxy state with N4-copper chelate heme/Cu complexes (Table 1) and contrasts with those of N3-copper chelate heme-peroxo-Cu complexes, which exhibit lower O−O stretching vibrations.[21] The 576 cm^{-1} isotope-sensitive band is attributable to the Fe−O_2 stretching vibration of a heme superoxide and shows the same value as that observed in EtCN solution. This rules out assignment as the ν_{Fe-O} of the peroxide because of splitting of the oxidation state marker band (ν_4) of the porphyrin at 1360 and 1366 cm^{-1} in the rR spectra (Figure 7). The ratio of the peroxide to superoxide as inferred from the intensity of the oxidation marker band is about 1:1. The EPR spectrum of the frozen sample of the oxy form reveals a Cu^{II} EPR signal of an intensity corresponding to ≈50% of that of its oxidized form at room temperature (Figure 5b), consistently with the results obtained from the rR experiments. From this it can

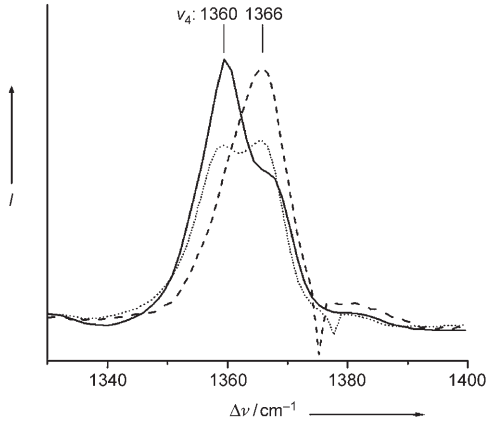

Figure 7. High-frequency resonance Raman spectra of oxy-**2b** (——) and oxy-**2a** (•••••) generated in CH_2Cl_2/7% EtCN at −100 °C with $^{16}O_2$. Oxy-**2a** generated in EtCN (-----) at −80 °C with $^{16}O_2$; conditions: 413 nm excitation, 25 mW.

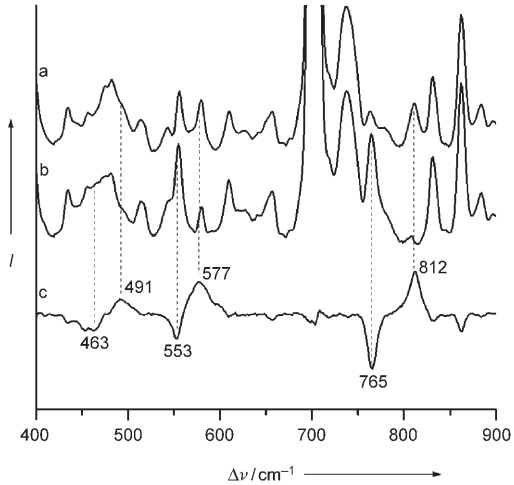

Figure 9. Resonance Raman spectra of oxy-**2b** formed from $^{16}O_2$ (a) and $^{18}O_2$ (b). c) Difference spectrum [a) minus b)]. Conditions: CH_2Cl_2/7% EtCN, −100 °C, excitation at 413 nm, 25 mW.

be inferred that the oxygenation reaction of **2a** in CH_2Cl_2/7% EtCN at low temperature produces mixtures of [heme-peroxo-copper(II)] and [heme-superoxo, copper(II)] intermediates in equivalent amounts.

Deprotonation of the crosslinked phenol moiety of compound **2a** by treatment with Na_2CO_3 solution yields compound **2b**. Notably, its oxygenation reaction results in the formation of peroxide as the major dioxygen adduct with the proportion of the superoxide species decreasing significantly (peroxo/superoxo ≈70:30). Oxygenation of **2b** in CH_2Cl_2/7% EtCN solution at −100 °C produces UV/visible spectral changes similar to those seen with **2a**, while a small but apparent difference is observable in the Q-band region, which shows new bands at 546 nm ($\varepsilon = 5400\ M^{-1}cm^{-1}$) and 570 nm (sh) with decreased absorption coefficients (Figure 8). The rR spectrum of the oxy form shows obvious Raman enhancement of the O–O stretching vibration, which appears at 812 cm^{-1} with $^{16}O_2$ and shifts to 765 cm^{-1} upon substitution with $^{18}O_2$ (Figure 9). In the low-frequency region, a new isotope-sensitive band at 491 ($^{16}O_2$)/463 cm^{-1} ($^{18}O_2$) is observable in addition to the 577 ($^{16}O_2$)/553 cm^{-1} ($^{18}O_2$) band arising from the Fe–O_2 stretching vibration of a heme superoxide. Although not well defined from the background, this isotope-sensitive band is indeed present in difference spectra from repeated experiments. The band at 491 cm^{-1} ($\Delta^{18}O_2 = -28$ cm^{-1}) resembles that of the reported ν_{Cu-O} mode in binuclear copper peroxide adducts [ν_{Cu-O}: 488 cm^{-1} ($\Delta^{18}O_2 = -24$ cm^{-1})],[22] whereas its value is lower than that of the reported ν_{Fe-O} in heme-O_2-Cu peroxides [ν_{Fe-O}: 529 cm^{-1} ($\Delta^{18}O_2 = -21$ cm^{-1})].[10] As a result, it may tentatively be assigned to the ν_{Cu-O} mode of the newly formed peroxide. The main porphyrin oxidation marker band (ν_4) appears at 1360 cm^{-1} with a small shoulder at 1366 cm^{-1} (Figure 7), which suggests that the dioxygen adducts are dominated by the peroxide species in the solution. The spin state marker band (ν_2) of the porphyrin appears at 1554 cm^{-1}, consistent with the presence of five-coordinate high-spin ferric heme. This peroxide species has poorer thermal stability than its tetradentate counterpart [($L^{N4\text{-}OH}$)Cu^{II}-O_2-Fe^{III}(TMP)]$^+$ (**1a**-O_2), requiring temperatures below −75 °C in CH_2Cl_2/7% EtCN solution and its O–O stretching frequency shifts by 13 cm^{-1}. Only a weak Cu^{II} signal is observable in the EPR spectrum of the frozen sample of the oxy form (Figure 5a), providing further evidence for the existence of a dioxygen-bridged peroxide species as the main adduct. The EPR results also rule out the presence of a side-on η^2-peroxo dioxygen heme/Cu^{II} adduct because the side-on η^2-peroxo dioxygen heme adduct usually displays a strong EPR marker signal at $g = 4.2$.[23]

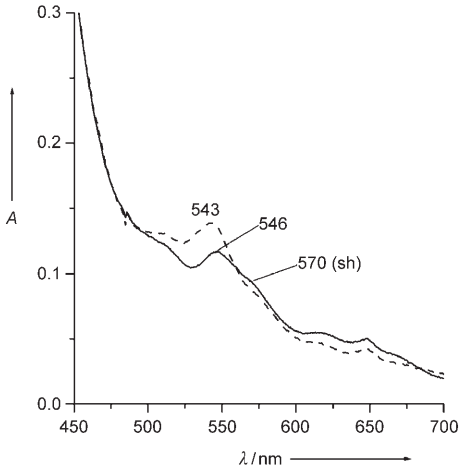

Figure 8. UV/visible spectra of oxy-**2a** (-----) and oxy-**2b** (——) generated in CH_2Cl_2/7% EtCN solution at −100 °C.

From all of these spectroscopic observations, we conclude that the oxygenation reaction of the deprotonated-hydroxy model compound **2b** in CH_2Cl_2/7% EtCN solution yields a bridged peroxide [($L^{N3\text{-}ONa}$)Cu^{II}-O_2-Fe^{III}(TMP)]$^+$ as the main component and a heme superoxide as a minor component. It is noteworthy that the frequency of the O–O stretching vibration (812 cm^{-1}) of this newly formed peroxide is distin-

guishable from those of the tridentate copper chelate heme-peroxo-Cu complexes, which exhibit lower ν_{O-O} values (740–770 cm^{-1}) (Table 1), while its value resembles that of the heme-peroxo-Cu complexes with tetradentate copper chelate [ν_{O-O}: ≈800 cm^{-1}]. As the inclination of Cu^{II} forms is to form five-coordinate complexes, tetradentate ligation of Cu^{I} limits the binding of dioxygen to an end-on fashion, while tridentate ligation of Cu^{I} favors the side-on binding of dioxygen.[24] It is most likely that the dioxygen binding mode for $[(L^{N3\text{-}ONa})Cu^{II}\text{-}O_2\text{-}Fe^{III}(TMP)]^+$ adopts a different $\mu\text{-}\eta^1\text{:}\eta^2$ pattern with η^1 to Fe and η^2 to Cu. Nevertheless, these experimental results cannot rule out another outcome in which dioxygen adopts the same binding configuration as in N4-copper chelate heme-peroxo-Cu complexes ($\mu\text{-}\eta^1\text{:}\eta^2$ with η^2 to Fe and η^1 to Cu), with the copper(II) site coordinated by an additional solvent molecule such as EtCN (Figure 10).

Oxygenation of the MOM-protected compound **2c** occurs in a similar manner to that of **2a**. In EtCN solvent at −80 °C, the oxygenation reaction produces a heme superoxide as the only observable dioxygen adduct, whereas in CH_2Cl_2/7 % EtCN solution (Figure S6 and Figure S7, Supporting Information) it yields both the heme superoxide [ν_{Fe-O_2}: 578 ($^{16}O_2$)/552 cm^{-1} ($^{18}O_2$)] and the peroxide species [ν_{O_2}: 812 ($^{16}O_2$)/765 cm^{-1} ($^{18}O_2$)] in proportions of about 55 and 45 %, respectively.

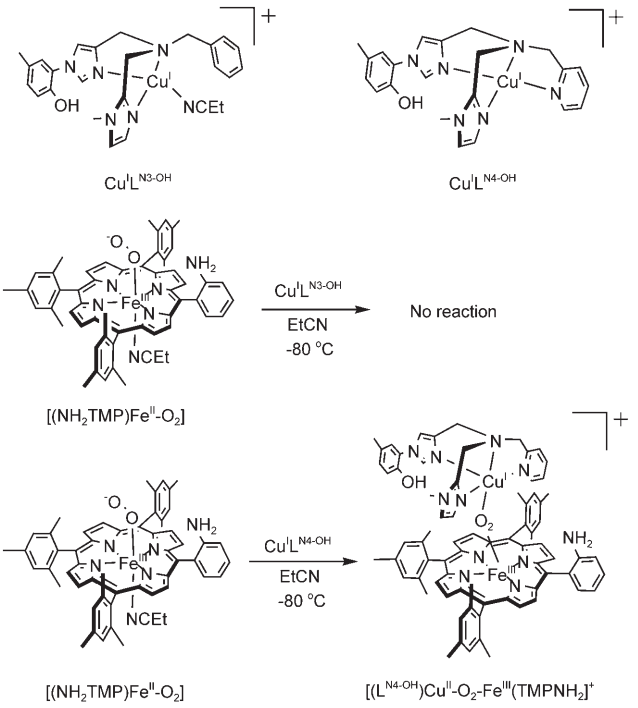

Scheme 4. Reaction behavior of the untethered heme superoxide $[(NH_2TMP)Fe^{III}\text{-}(O_2^-)]$ with the copper(I) components $[Cu^IL^{N3\text{-}OH}]^+$ and $[Cu^IL^{N4\text{-}OH}]^+$.

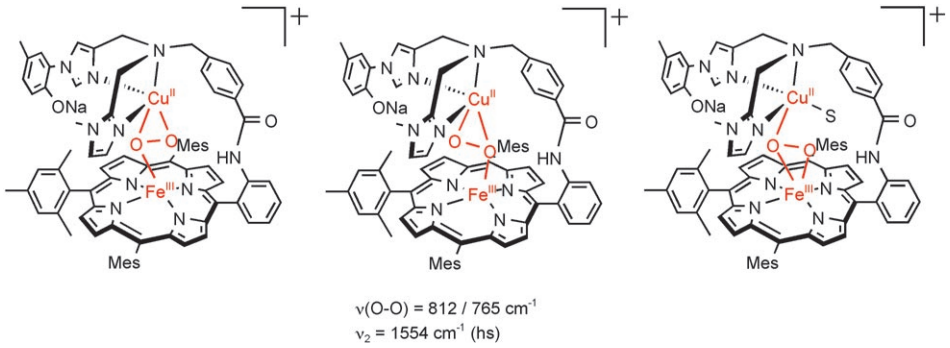

Figure 10. Possible dioxygen binding modes for the peroxide $[(L^{N3\text{-}ONa})Cu^{II}\text{-}O_2\text{-}Fe^{III}(TMP)]^+$.

Reactions between untethered heme superoxide and Cu^I complexes: The experimental results demonstrate that the oxygenation of the N3-copper chelate C*c*O model **2a** differs significantly from that of its tetradentate counterpart **1a**. To increase our understanding of the unusual oxygenation behavior of **2a** further, we studied some preliminary reactions of untethered heme superoxide $[(NH_2TMP)Fe^{III}\text{–}(O_2^-)]$, which is formed from the oxygenation of the lower part of **1a** or **2a**, with copper(I) components $[Cu^IL^{N4\text{-}OH}]^+$ and $[Cu^IL^{N3\text{-}OH}]^+$, which correspond to the copper moieties of the tethered models **1a** and **2a**, respectively (Scheme 4). Oxygenation of $(NH_2TMP)Fe^{II}$ in EtCN at −80 °C produced a superoxide with electronic absorption maxima at 415, 543, and 582 nm. After removal of excess dioxygen, one equivalent of the copper(I) complex $[Cu^IL^{N3\text{-}OH}]^+$ was added to the solution, during which the absorption maxima remain unchanged (Figure 11 a). Upon addition of one equivalent of $[Cu^IL^{N4\text{-}OH}]^+$ to the heme superoxide solution, however, a new species is generated, with UV/Vis features (EtCN, λ_{max} = 421, 567, 616 nm, Figure 11 b) very similar to those of the peroxide $[(L^{N4\text{-}OH})Cu^{II}\text{-}O_2\text{-}Fe^{III}\text{-}(TMP)]^+$ formed with the tethered model **1a** (MeCN, λ_{max} = 421, 558, 614 nm). These results clearly show that the tridentate chelated copper(I) complex $[Cu^IL^{N3\text{-}OH}]^+$ cannot reduce the corresponding heme superoxide and that the formation of the untethered heme-peroxo-copper species is only observed with the tetradentate-ligated copper(I) complex $[Cu^IL^{N4\text{-}OH}]^+$. This is interpreted in terms of a tridentate chelated copper(I) complex usually being a poor reductant, while a tetradentate ligand makes its copper(I) complex a stronger reductant, facilitating binding and reaction with the heme superoxide, as is further manifested by the Cu^{II}/Cu^I redox potentials of these two complexes ($[Cu^IL^{N3\text{-}OH}]^+$: $E_{1/2}$ = −0.32 V; $[Cu^IL^{N4\text{-}OH}]^+$: $E_{1/2}$ = −0.47 V vs Fc/Fc^+ in MeCN). Thus, the tridentate-chelated copper(I) complex $[Cu^IL^{N3\text{-}OH}]^+$, the upper part of **2a**, does not react with the heme superoxide $[(NH_2TMP)Fe^{III}\text{-}(O_2^-)]$, a moiety of the dioxygen adduct formed with the heme part of **2a**. Meanwhile, the complex readily reacts with dioxygen. It is notable that the oxygena-

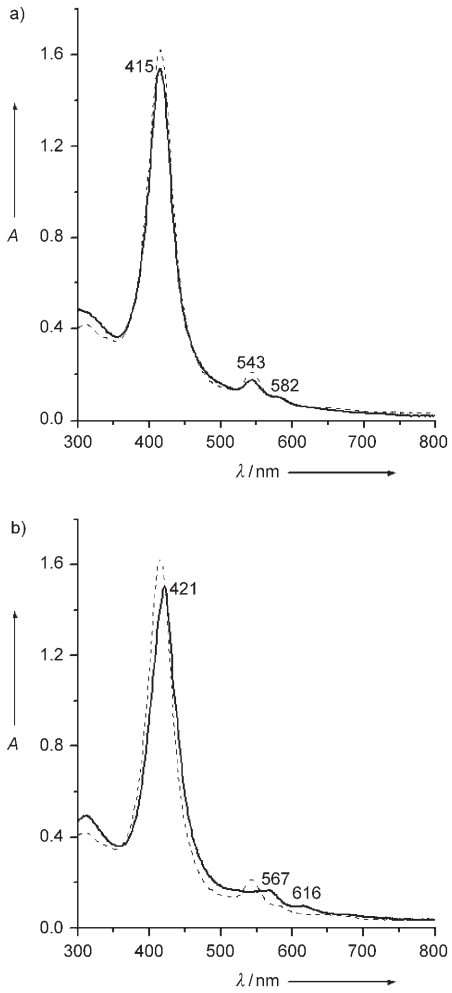

Figure 11. a) UV/visible spectrum of the superoxo compound $[(NH_2TMP)Fe^{II}–O_2]$ (-----) and the resultant spectrum after addition of $Cu^{I}L^{N3\text{-}OH}$ (——). b) UV/visible spectrum of the superoxo compound $[(NH_2TMP)Fe^{II}–O_2]$ (-----) and the resultant spectrum after addition of $Cu^{I}L^{N4\text{-}OH}$ (——).

tion reaction of $[Cu^{I}L^{N3\text{-}OH}]^{+}$ in EtCN is strongly suppressed relative to that in CH_2Cl_2, which would usually be expected when dioxygen binds to a tridentate-ligated copper(I) complex.[21a–b,25]

Possible mechanism for dioxygen binding to model compounds: From these experimental observations of the tethered and untethered systems, stepwise binding of dioxygen to the N3-copper chelate C*c*O model **2a** is proposed (Scheme 5). When oxygenation of **2a** is carried out in EtCN, binding of O_2 to the $[Cu^{I}L^{N3\text{-}OH}]^{+}$ site is significantly suppressed by the solvent EtCN molecules and a transient species $[L^{N3\text{-}OH}Cu^{I}\cdots(O_2^{-})\text{-}Fe^{III}TMP]^{+}$ may be produced, in which the copper portion $[Cu^{I}L^{N3\text{-}OH}]^{+}$ cannot react further with the corresponding superoxide because of its weak reducibility. Consequently, copper(I) is directly oxidized to copper(II) by the existing excess amounts of dioxygen, until it finally produces the heme superoxide, with the copper part oxidized to Cu^{II}. On the other hand, when the oxygenation takes place in CH_2Cl_2/7% EtCN solution, binding of O_2 both to the copper(I) site and to the lower ferrous heme proceeds competitively and statistically generates two transient species: $[L^{N3\text{-}OH}Cu^{I}\cdots(O_2^{-})\text{-}Fe^{III}TMP]^{+}$ and $[L^{N3\text{-}OH}\text{-}Cu^{II}\text{-}(O_2^{-})\cdots Fe^{II}TMP]^{+}$. The former species ultimately produces the heme superoxide, leaving the cupric component unbound, and the latter species—in which the side-on-bound $Cu^{II}(O_2^{-})$ moiety can further react with the lower ferrous heme—eventually yields the bridged peroxide. Deprotonation of the crosslinked phenol moiety yields a monoanionic ligand that endows the copper(I) complex with enhanced O_2 reactivity. As a result, the relative proportion of the second transient species increases and the formation of a bridged heme-O_2-Cu adduct rises as observed experimentally. In the case of **1a**, initial O_2 binding may occur either at the $Cu^{I}L^{N4\text{-}OH}$ site or at the ferrous heme moiety, to generate the resultant transient species $[L^{N4\text{-}OH}Cu^{I}\cdots(O_2^{-})\text{-}Fe^{III}TMP]^{+}$ and $[L^{N4\text{-}OH}Cu^{II}\text{-}(O_2^{-})\cdots Fe^{II}TMP]^{+}$, either of which will progress to the formation of the dioxygen-bridged peroxide product.

With regard to the possible roles of the crosslinked His-Tyr moiety, our very recent study on model complexes of the Cu_B site of C*c*O reveals that the imidazole–phenol covalent linkage has only a minor effect on the electronic structure of the phenoxyl radical. It appears that its role is more likely to be structural rather than its acting as a provider of the fourth electron in the dioxygen reduction process.[9a] Since it has been proposed that association of dioxygen with Cu_B^{I} prior to binding to heme a_3 might occur during the early stage of the oxygenation reaction with reduced C*c*O,[26] this model study leads us to propose that the deprotonated crosslinked His-Tyr, identified by Yoshikawa et al.[3a] in the fully oxidized state of the enzyme, may serve to enhance the

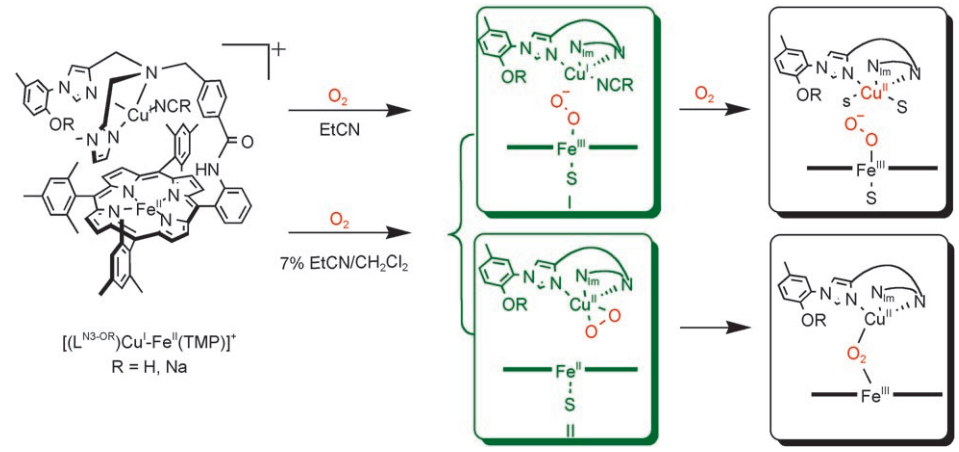

Scheme 5. Proposed stepwise binding of dioxygen to the model compounds.

O_2 affinity of Cu_B^I site at an early stage of the O_2 binding process.

Conclusion

Heterobinucleating ligands composed of a porphyrin together with either a tetradentate N4-copper chelate or a tridentate N3-copper chelate with a crosslinked His-Tyr mimic, and their corresponding heme-copper complexes $[(L^{N4\text{-}OH})Cu^{I}\text{-}Fe^{II}(TMP)]^+$ (**1a**) and $[(L^{N3\text{-}OH})Cu^{I}\text{-}Fe^{II}(TMP)]^+$ (**2a**), respectively, have been designed and synthesized as model compounds of the active site of cytochrome *c* oxidase. These two models showed distinct oxygenation reactions at low temperature. Oxygenation of the tetradentate model **1a** both in MeCN and in other solvents produced a low-temperature-stable dioxygen-bridged peroxide $[(L^{N4\text{-}OH})Cu^{II}\text{-}O_2\text{-}Fe^{III}(TMP)]^+$ with an O–O stretching vibration at 799 cm^{-1}. Oxygenation of the tridentate model **2a** in EtCN solution, however, generated a heme superoxide species $[(TMP)Fe^{III}\text{-}(O_2^-)\cdots Cu^{II}(L^{N3\text{-}OH})]$ with the copper moiety oxidized to copper(II). Moreover, the coexistence of a heme superoxide $[(TMP)Fe^{III}(O_2^-)\cdots Cu^{II}(L^{N3\text{-}OH})]$ and a bridged peroxide $[(L^{N3\text{-}OH})Cu^{II}\text{-}O_2\text{-}Fe^{III}(TMP)]^+$ species in equivalent amounts was observed when the oxygenation reaction of **2a** was carried out in CH_2Cl_2/7% EtCN. An increase in the ratio of the peroxide ($\approx$70%) to superoxide ($\approx$30%) was found when the crosslinked phenol moiety of **2a** was deprotonated, producing a bridged peroxide complex $[(L^{N3\text{-}ONa})Cu^{II}\text{-}O_2\text{-}Fe^{III}(TMP)]^+$ as the main dioxygen intermediate, with the $\nu_{O\text{–}O}$ frequency at 812 cm^{-1}. Observations from the reactions of the untethered copper moieties of $[Cu^{I}L^{N4\text{-}OH}]^+$ and $[Cu^{I}L^{N3\text{-}OH}]^+$ with the untethered heme superoxide $[(NH_2TMP)Fe^{III}\text{-}(O_2^-)]$ demonstrated that the tridentate copper(I) component $[Cu^{I}L^{N3\text{-}OH}]^+$ did not react with the corresponding heme superoxide, whereas the tetradentate counterpart tended to react and yield the resultant dioxygen-bridged peroxide, which can also be generated with the tethered model **1a**. The different oxygenation behavior exhibited by the tri- and tetradentate copper chelate heme/copper models is explained by the tricoordinated copper(I) site having a weak reducibility and decreased O_2 reactivity relative to those of the tetracoordinated complex. A stepwise process of binding of dioxygen to the N3-copper chelate heme/copper model **2a** has been proposed on the basis of the experimental observations with the tethered and untethered systems, with initial association of dioxygen to the copper site occurring en route to the formation of the dioxygen-bridged heme-peroxo-Cu intermediate.

Experimental Section

Instruments and methods: ^1H NMR and ^{13}C NMR spectra were recorded on a JEOL LMX-GX 400 (400 MHz) spectrometer. Chemical shifts were referenced to the residual solvent signal. Electrospray ionization mass (ESI-MS) spectra were obtained on a Perkin–Elmer Sciex API-300 mass spectrometer. Scanning was in 0.1 Dalton steps with a 10 ms dwell time per step. The orifice voltage was controlled from −20 to +180 V, dependent on the intensity of TIC. High-resolution mass (HR-MS) spectra were recorded on a JEOL LMS-HX-110 spectrometer with 3-nitrobenzyl alcohol (NBA) as a matrix. The UV/Vis electronic spectra were recorded on a Hamamatsu PMA-11 CCD spectrophotometer with a Photal MC-2530 (D_2/W_2) as a light source. The temperature was controlled with a NESLAB ULT-95 low=temperature circulator. Infrared spectra were recorded on a BIO-RAD FTS-6000 spectrometer. EPR spectra were obtained at 77 K in 5.0 mm diameter ESR quartz tubes on a JEOL JES-TE 300 spectrometer. The magnetic field was calibrated from the hyperfine coupling constants (hfccs) of Mn^{II} ion doped in MgO powder (86.9 Gauss). The UV/Vis electronic spectra were recorded on a Hamamatsu PMA-11 CCD spectrophotometer with a Photal MC-2530 (D_2/W_2) as a light source. The temperature was controlled with a NESLAB ULT-95 low-temperature circulator.

Resonance Raman (rR) spectra were obtained on a SpectraPro-300i spectrometer (Acton Research) with a 2400-groove grating, a Beamlok 2060 Kr ion laser (Spectra-physics), a holographic Supernotch filter (Kaiser Optical Systems), and an LN-1100PB CCD detector (Princeton Instruments) cooled with liquid N_2. Spectra were collected in spinning cells (2.0 cm diameter, 1500 rpm) at an excitation wavelength λ_{ex}= 413.1 nm, 90° scattering geometry, and 5 min data accumulation. Peak frequencies were calibrated relative to indene and CCl_4 standards (accurate to $\pm$1 cm^{-1}). During each Raman experiment, UV/Vis spectra were simultaneously collected on a PMA-11 CCD spectrophotometer (Hamamatsu) with a Photal MC-2530 (D_2/W_2) light source (Otsuka Electronic Co.).

The cyclic voltammetry (CV) measurements were performed on a BAS 100B/W electrochemical analyzer in anhydrous MeCN containing $[Bu_4N][ClO_4]$ (0.1 M) as a supporting electrolyte. A glassy carbon working electrode was polished with a polishing alumina suspension and rinsed with MeCN before use. A Pt wire was used as counter electrode. A nonaqueous Ag/Ag^+ electrode was used as reference electrode and the potentials were determined by use of the ferrocene/ferricenium (Fc/Fc^+) couple as a reference. Electrochemical measurements were carried out at 25 °C under an atmospheric pressure of N_2 in a glovebox (M. Braun 150B-G-II).

Oxygenation reaction: Dry O_2 gas was introduced through molecular sieves by O_2 line into a degassed solution of the model compound ($\approx10^{-4}$ M) in a 0.2 cm UV cuvette. The spectral changes were monitored with a UV/Vis spectrometer. Oxygenation of the sample solution ($\approx10^{-5}$ M) for ESI-MS measurement was carried out in the same way in a 1.0 cm UV cuvette, which was capped with a three-way stopcock sealed with rubber septa and kept in a handmade cell box for UV/Vis measurements, a Teflon capillary tube being immersed into the resultant solution for ESI-MS measurement. The solution was introduced into the ion-spray ionization port of the spectrometer by application of appropriate N_2 pressure. The sample for rR measurement was prepared by injection of dry O_2 gas (10 mL) by syringe into the solution of the model compound ($\approx10^{-4}$ M) in a cylindrical Raman cell at low temperature. The sample for EPR measurement was prepared as follows: in a glovebox, a solution of the model compound ($\approx10^{-3}$ M) was transferred to an EPR tube. The tube was capped with a rubber septum and moved out of the glovebox and kept in a cold bath (liq. N_2/ethanol) at −100 to −80 °C (for **1a** and **1b**, at −30 °C). Dry O_2 gas was introduced by syringe and the resultant oxygenated solution was allowed to stand at this temperature for 20 min, after which the solution was frozen in liquid N_2 and excess O_2 was removed under vacuum.

Reactions of $Cu^{I}L^{N3\text{-}OH}$ and $Cu^{I}L^{N4\text{-}OH}$ with the heme superoxide $[(NH_2TMP)Fe^{III}\text{-}(O_2^-)]$: The complexes of $Cu^{I}L^{N3\text{-}OH}$ and $Cu^{I}L^{N4\text{-}OH}$ were prepared in situ in a glovebox by mixing compound $L^{N3\text{-}OH}$ (or $L^{N4\text{-}OH}$) and $[Cu^{I}(CH_3CN)_4](TfO^-)$ in 1:1 ratio in oxygen-free and dry EtCN, and the resultant solutions of the Cu^{I} complexes were stirred for 30 min at RT and transferred to a volumetric flask as a stock solution. Oxygenation of the $[(NH_2TMP)Fe^{II}]$ in EtCN at −80 °C to generate the heme superoxide $[(NH_2TMP)Fe^{III}\text{-}(O_2^-)]$ was carried out in the same way as described above and excess O_2 was removed from the UV cuvette by evacuation of

the headspace and backfilling with N_2 (×5). One equivalent amount of Cu^I complex was then added to the resultant solution and its UV/Vis spectral changes were recorded.

Materials: All reagents and solvents were obtained commercially and were used without further purification unless otherwise noted. Triethylamine was dried with KOH and distilled before use. Chloroform was distilled over K_2CO_3. Acetone was distilled twice from anhydrous calcium sulfate and stored for no longer than two weeks before use. *N*,*N*-Dimethylformamide (DMF) was distilled from CaH_2 under reduced pressure and kept over 4 Å molecular sieves. Diethyl ether (Et_2O) was predried over $CaCl_2$ and distilled from Na/benzophenone under N_2. Tetrahydrofuran (THF) was predried over KOH and distilled from Na/benzophenone under N_2. Dichloromethane (CH_2Cl_2) was stirred with concentrated H_2SO_4 for several days and dried over K_2CO_3, and was then distilled from CaH_2 under N_2. Synthetic-grade acetonitrile (MeCN) was distilled from P_2O_5 and redistilled from CaH_2. Dry MeCN for spectroscopic measurements was further purified as follows: the double-distilled synthetic-grade MeCN was degassed three times by the freeze-thaw method, and was stirred over KO_2 (Aldrich) for ca. 1 h and then passed through activated alumina (Wako), which had previously been dried at 220 °C under vacuum for 10 h. Subsequently, it was again degassed three times by freeze-thaw technique. Propionitrile (EtCN) was treated as the same way as MeCN. The other degassed solvents were also treated by the freeze–thaw method. Preparation and handling of air-sensitive materials were carried out under N_2 in a glovebox (M. Braun 150B-G-II) fitted with a circulating purifier (O_2, H_2O < 1 ppm).

Syntheses: (1-Methyl-1*H*-imidazol-4-yl)methanol hydrochloride,[27] 2-(aminomethyl)-1-methyl-1*H*-imidazole dihydrochloride (**8**),[28] 6-(chloromethyl)nicotinic acid methyl ester hydrochloride (**10**),[29] [Cu(OH)TMEDA]$_2$Cl$_2$[13] and [Cu^I(CH$_3$CN)$_4$](TfO$^-$)[30] were prepared by literature procedures. The preparation of (2-[10,15,20-tris-(2,4,6-trimethylphenyl)porphyrin-5-yl]phenylamine (TMPNH$_2$, **16**) and insertion of iron into the porphyrin ([Fe^{II}(TMPNH$_2$)]$^+$) were by established methods.[31]

2-Bromo-1-methoxymethoxy-4-methylbenzene: A mixture of 2-bromo-*p*-cresol (7.5 g, 40 mmol) and K_2CO_3 (13.8 g, 100 mmol) in dry acetone (100 mL) was stirred at RT for 1 h, and chloromethyl methyl ether (3.8 mL, 50 mmol) was added dropwise to the mixture. The mixture was stirred at RT overnight. After filtration, water (80 mL) was added to the filtrate and the mixture was extracted with ethyl acetate (3×80 mL). The combined organic phase was washed with HCl (1.0 M) and brine and then dried over anhydrous Na_2SO_4. Solvent removal gave the methoxymethyl derivative as a colorless oil (8.6 g, 93 %). ^{1}H NMR (400 MHz, $CDCl_3$): δ = 7.37 (s, 1H), 7.04 (s, 2H), 5.21 (s, 2H), 3.52 (s, 3H), 2.28 ppm (s, 3H); ^{13}C NMR (100 MHz, $CDCl_3$): δ = 151.34, 133.48, 132.78, 128.76, 116.14, 112.49, 95.16, 56.19, 20.18 ppm.

2-Methoxymethoxy-5-methyl-phenylboronic acid (3): *n*-Butyllithium (1.6 M in hexane, 25.0 mL, 40 mmol) was added to a cold (−70 °C) solution of 2-bromo-1-methoxymethoxy-4-methylbenzene (6.93 g, 30 mmol) in dry Et_2O (300 mL). The resulting solution was stirred for 2 h and a white precipitate appeared. The mixture was again cooled to −70 °C and trimethyl borate (4.5 mL, 40 mmol) was slowly added. Stirring was continued for 6 h at room temperature, before hydrolysis with a hydrochloric acid solution (1.0 M) and stirring for further 0.5 h at room temperature. The ethereal extract was washed with water (100 mL) and dried ($MgSO_4$). Removal of solvents under reduced pressure followed by purification by recrystallization from Et_2O/hexane afforded the pure arylboronic acid as colorless crystals (3.9 g, 70 %). ^{1}H NMR (400 MHz, $CDCl_3$): δ = 7. 66 (s, 1H), 7.23 (d, *J* = 8.0 Hz, 1H), 7.03 (d, *J* = 8.0 Hz, 1H), 5.99 (s, 2H), 5.27 (s, 2H), 3.50 (s, 3H), 2.31 ppm (s, 3H); ^{13}C NMR (100 MHz, $CDCl_3$): δ = 160.16, 137.02, 136.99, 133.20, 131.35, 113.24, 94.67, 56.39, 20.46 ppm.

4-(*tert*-Butyldiphenylsilanyloxymethyl)-1*H*-imidazole (4): 4-(Hydroxymethyl)imidazole hydrochloride (2.68 g, 20 mmol), TBDPSC (6.68 g, 24 mmol), and imidazole (3.44 g, 50 mmol) were dissolved in DMF (10 mL) and the mixture was stirred under nitrogen at 50 °C for 24 h. Water (60 mL) was added to the mixture, which was extracted with $CHCl_3$ (3×80 mL). The combined organic layer was washed several times with water (3×100 mL) and dried (Na_2SO_4), and solvent removal afforded the crude compound, which was purified by silica gel column chromatography ($CHCl_3$/MeOH 15:1) to give the product as a white solid (6.2 g, 92 %). ^{1}H NMR (400 MHz, $CDCl_3$): δ = 7.85 (s, 1H), 6.94 (s, 1H), 4.72 (s, 2H), 0.90 (s, 9H), 0.07 ppm (s, 6H); ^{13}C NMR (100 MHz, $CDCl_3$): δ = 135.42, 134.91, 134.86, 133.32, 129.60, 127.60, 59.26, 26.84, 19.25 ppm; ESI-MS: *m*/*z*: 337.2 [*M*+H]$^+$; HR-MS (FAB, NBA): *m*/*z*: calcd for $C_{20}H_{25}N_2OSi$: 337.1736; found: 337.1736 [*M*+H]$^+$.

4-(*tert*-Butyldiphenylsilanyloxymethyl)-1-(2-methoxymethoxy-5-methylphenyl)-1*H*-imidazole (5): A mixture of arylboronic acid **3** (2.2 g, 11 mmol), Im-TBDPS **4** (3.4 g, 10 mmol), and [Cu(OH)TMEDA]$_2$Cl$_2$ (0.46 g, 1 mmol) in dry dichloromethane (60 mL) was vigorously stirred under dioxygen at room temperature for 48 h. The reaction mixture was filtered, the filtrate was concentrated, and the residue was purified by silica gel column chromatography (C-200, ethyl acetate/hexane 2:1) to give the *N*-arylimidazole **5a** (3.6 g, 75 %). ^{1}H NMR (400 MHz, $CDCl_3$): δ = 7.86 (s, 1H), 7.72 (d, *J* = 8.0 Hz, 4H), 7.43–7.36 (m, 6H), 7.20 (d, *J* = 8.0 Hz, 1H), 7.15 (d, *J* = 8.0 Hz, 1H), 7.11 (s, 1H), 7.08 (s, 1H), 5.12 (s, 2H), 4.86 (s, 2H), 3.37 (s, 3H), 2.36 (s, 3H), 1.11 ppm (s, 9H); ^{13}C NMR (100 MHz, $CDCl_3$): δ = 147.51, 141.73, 136.75, 135.13, 133.25, 131.76, 129.17, 128.72, 127.22, 126.95, 125.52, 116.90, 116.19, 94.91, 60.81, 55.77, 26.56, 20.11, 18.97 ppm; ESI-MS: *m*/*z*: 487.2 [*M*+H]$^+$; HR-MS (FAB, NBA): *m*/*z*: calcd for $C_{29}H_{35}N_2O_3Si$: 487.2417; found: 487.2410 [*M*+H]$^+$.

Compound **5b** (0.3 g, 7 %) was also obtained. ^{1}H NMR (400 MHz, $CDCl_3$): δ = 7.63 (s, 1H), 7.50 (d, *J* = 8.0 Hz, 4H), 7.39 (t, 2H), 7.34 (t, 4H), 7.22 (d, *J* = 8.0 Hz, 1H), 7.19 (s, 1H), 7.16 (d, *J* = 8.0 Hz, 1H), 7.05 (s, 1H), 4.95 (s, 2H), 4.51 (s, 2H), 3.20 (s, 3H), 2.31 (s, 3H), 0.91 ppm (s, 9H); ^{13}C NMR (100 MHz, $CDCl_3$): δ = 149.70, 138.65, 135.13, 132.71, 131.86, 131.50, 130.17, 129.35, 129.02, 127.76, 127.36, 125.63, 115.74, 94.81, 60.06, 55.56, 26.34, 20.13, 18.83 ppm; ESI-MS: *m*/*z*: 487.2 [*M*+H]$^+$; HR-MS (FAB, NBA): *m*/*z*: calcd for $C_{29}H_{35}N_2O_3Si$: 487.2417; found: 487.2413 [*M*+H]$^+$.

[1-(2-Methoxymethoxy-5-methylphenyl)-1*H*-imidazol-4-yl]methanol (6): Tetrabutylammonium fluoride in THF (1.0 M, 30 mL) was added to a solution of **5a** (4.90 g, 10 mmol) in THF (25 mL) and the mixture was stirred at room temperature overnight. Water (40 mL) was added to the solution, which was extracted with $CHCl_3$ (3×50 mL). The combined organic layer was washed with water (3×80 mL) and dried over anhydrous Na_2SO_4, the solvent was removed under reduced pressure, and the resultant residue was purified by silica gel column chromatography with $CHCl_3$/CH_3OH 15:1. The product was isolated as a pale yellow oil (2.30 g, 93 %). ^{1}H NMR (400 MHz, $CDCl_3$): δ = 7.86 (s, 1H), 7.15–7.20 (m, 3H), 7.10 (s, 1H), 5.13 (s, 2H), 4.70 (s, 2H), 3.42 (s, 3H), 2.34 ppm (s, 3H); ^{13}C NMR (100 MHz, $CDCl_3$): δ = 147.76, 141.81, 137.41, 132.04, 129.15, 126.73, 125.80, 117.38, 116.25, 95.08, 57.55, 56.11, 20.34 ppm; ESI-MS: *m*/*z*: 249.1 [*M*+H]$^+$; HR-MS (FAB, NBA): *m*/*z*: calcd for $C_{13}H_{17}N_2O_3$: 249.1239; found: 249.1240 [*M*+H]$^+$.

1-(2-Methoxymethoxy-5-methylphenyl)-1*H*-imidazole-4-carbaldehyde (7): A mixture of compound **6** (2.48 g, 10 mmol) and activated MnO_2 (50 mmol) in chloroform was heated at reflux for 3 d. The reaction mixture was allowed to cool to room temperature and filtered, and the filtrate was concentrated. The residue was purified by silica gel column chromatography with $CHCl_3$/CH_3OH 15:1 to give the title compound (2.1 g, 85 %). ^{1}H NMR (400 MHz, $CDCl_3$): δ = 9.95 (s, 1H), 7.90 (s, 1H), 7.85 (s, 1H), 7.20 (dd, *J* = 8.0 and 3.6 Hz, 2H), 7.12 (s, 1H), 5.14 (s, 2H), 3.37 (s, 3H), 2.35 ppm (s, 3H); ^{13}C NMR (100 MHz, $CDCl_3$): δ = 186.09, 147.91, 141.83, 139.14, 132.38, 130.47, 125.80, 125.69, 125.59, 116.32, 95.24, 56.36, 20.43 ppm; ESI-MS: *m*/*z*: 247.1 [*M*+H]$^+$; HR-MS (FAB, NBA): *m*/*z*: calcd for $C_{13}H_{15}N_2O_3$: 247.1083; found: 247.1080 [*M*+H]$^+$.

[1-(2-Methoxymethoxy-5-methylphenyl)-1*H*-imidazol-4-ylmethyl](1-methyl-1*H*-imidazol-2-ylmethyl)amine (9): 2-(Aminomethyl)-1-methyl-1*H*-imidazole dihydrochloride (**8**, 1.85 g, 10 mmol) and aldehyde **7** (2.46 g, 10 mmol) were dissolved in dry methanol (100 mL). Triethylamine was added to neutralize the solution, which was kept at reflux under nitrogen for 8 h and then allowed to cool to room temperature. $NaBH_4$ was added to the cooled mixture, which was stirred overnight. Water was added to the solution, which was extracted with chloroform (3×80 mL). The combined organic layer was washed with water and dried over Na_2SO_4 and the residue was purified by silica gel column chro-

matography ($CHCl_3$/MeOH 15:1) to give the product (2.2 g, 65%). ^{1}H NMR (400 MHz, $CDCl_3$): δ = 7.72 (s, 1H), 7.16 (d, J = 8.0 Hz, 1H), 7.12 (d, J = 8.0 Hz, 2H), 7.08 (s, 1H), 6.93 (s, 1H), 6.82 (s, 1H), 5.11 (s, 2H), 3.96 (s, 2H), 3.85 (s, 2H), 3.70 (s, 3H), 3.38 (s, 3H), 2.32 ppm (s, 3H); ^{13}C NMR (100 MHz, $CDCl_3$): δ = 147.72, 146.24, 139.90, 137.36, 137.20, 132.07, 129.01, 126.89, 125.79, 120.98, 117.45, 116.29, 95.13, 56.15, 46.34, 44.72, 32.68, 20.43 ppm; ESI-MS: m/z: 342.1 $[M+H]^+$; HR-MS (FAB, NBA): m/z: calcd for $C_{18}H_{24}N_5O_2$: 342.1930; found: 342.1937 $[M+H]^+$.

6-{[[1-(2-Methoxymethoxy-5-methylphenyl)-1*H*-imidazol-4-ylmethyl](1-methyl-1*H*-imidazol-2-ylmethyl)amino]methyl}nicotinic acid methyl ester (12): 6-(Chloromethyl)nicotinic acid methyl ester hydrochloride (**10**, 1.22 g, 5.5 mmol) and triethylamine (1.53 mL, 11 mmol) were dissolved in dry acetonitrile (30 mL). Amine **9** (1.71 g, 5 mmol) was added to the mixture, which was stirred for several days at RT. The progress of the reaction was monitored by TLC. After completion of the reaction, the mixture was filtered and the precipitate was washed several times with dichloromethane. The combined organic layer was evaporated and the residue was passed through a silica gel column ($CHCl_3$/MeOH 15:1) to give the product as a pale yellow oil (1.5 g, 61%). ^{1}H NMR (400 MHz, $CDCl_3$): δ = 9.11 (s, 1H), 8.23 (d, J = 8.0 Hz, 1H), 7.75 (s, 1H), 7.61 (d, J = 8.0 Hz, 1H), 7.23 (s, 1H), 7.16 (d, J = 8.0 Hz, 1H), 7.11 (d, J = 8.0 Hz, 2H), 6.96 (s, 1H), 6.80 (s, 1H), 5.11 (s, 2H), 3.99 (s, 2H), 3.95 (s, 3H), 3.93 (s, 3H), 3.76 (s, 2H), 3.73 (s, 2H), 3.37 (s, 3H), 2.34 ppm (s, 3H); ^{13}C NMR (100 MHz, $CDCl_3$): δ = 165.58, 161.22, 150.78, 148.65, 144.56, 137.43, 137.30, 135.92, 132.11, 129.60, 126.53, 125.85, 126.48, 124.64, 122.08, 121.90, 119.76, 116.32, 95.18, 58.86, 56.04, 51.70, 49.54, 33.98, 20.41 ppm; ESI-MS: m/z: 491.2 $[M+H]^+$; HR-MS (FAB, NBA): m/z: calcd for $C_{26}H_{31}N_6O_4$: 491.2407; found: 491.2400 $[M+H]^+$.

6-{[[1-(2-Methoxymethoxy-5-methylphenyl)-1*H*-imidazol-4-ylmethyl](1-methyl-1*H*-imidazol-2-ylmethyl)amino]methyl}nicotinic acid (13): An aqueous solution of KOH (1.0 M) was added to a THF solution of the above ester **12** (2.45 g, 5 mmol). After stirring for 24 h, the solution was neutralized with aqueous HCl, and the solvent was removed under reduced pressure until dryness. The residue was then extracted with dichloromethane. Removal of the solvent gave the product as a pale yellow solid (2.0 g, 86%). ^{1}H NMR (400 MHz, $CDCl_3$): δ = 10.65 (br, 1H), 9.03 (s, 1H), 8.10 (d, J = 8.0 Hz, 1H), 7.98 (s, 1H), 7.45 (d, J = 8.0 Hz, 1H), 7.43 (s, 1H), 7.17 (d, J = 8.0 Hz, 2H), 7.12 (d, J = 8.0 Hz, 2H), 6.94 (s, 1H), 5.14 (s, 2H), 4.30 (s, 2H), 3.98 (s, 2H), 3.93 (s, 2H), 3.87 (s, 3H), 3.38 (s, 3H), 2.33 ppm (s, 3H); ^{13}C NMR (100 MHz, $CDCl_3$): δ = 167.97, 161.43, 150.26, 147.74, 144.70, 137.77, 137.49, 136.12, 132.30, 129.72, 126.86, 126.18, 125.84, 123.15, 122.82, 122.05, 120.10, 116.22, 95.21, 59.45, 56.33, 50.96, 48.81, 33.89, 20.45 ppm; ESI-MS: m/z: 477.3 $[M+H]^+$; HR-MS (FAB, NBA): m/z: calcd for $C_{25}H_{29}N_6O_4$: 477.2250; found: 477.2249 $[M+H]^+$.

4-{[[1-(2-Methoxymethoxy-5-methylphenyl)-1*H*-imidazol-4-ylmethyl]-(1-methyl-1*H*-imidazol-2-ylmethyl)amino]methyl}benzoic acid methyl ester (14): This compound was prepared in a similar way to compound **12**. Yield: 45%. ^{1}H NMR (400 MHz, $CDCl_3$): δ = 7.89 (d, J = 8.0 Hz, 2H), 7.68 (s, 1H), 7.36 (d, J = 8.0 Hz, 2H), 7.10–7.02 (m, 4H), 6.80 (s, 1H), 6.69 (s, 1H), 5.03 (s, 2H), 3.81 (s, 3H), 3.70 (s, 2H), 3.65 (s, 2H), 3.58 (s, 2H), 3.53 (s, 3H), 3.28 (s, 3H), 2.26 ppm (s, 3H); ^{13}C NMR (100 MHz, $CDCl_3$): δ = 166.70, 147.65, 145.08, 144.66, 137.72, 137.12, 132.03, 129.17, 129.02, 128.60, 128.41, 126.86, 126.73, 125.74, 121.32, 119.09, 116.27, 95.09, 57.38, 56.06, 51.80, 51.01, 50.14, 32.76, 20.31 ppm; ESI-MS: m/z: 490.2 $[M+H]^+$; HR-MS (FAB, NBA): m/z: calcd for $C_{27}H_{32}N_5O_4$: 490.2454; found: 490.2450 $[M+H]^+$.

4-{[[1-(2-Methoxymethoxy-5-methylphenyl)-1*H*-imidazol-4-ylmethyl](1-methyl-1*H*-imidazol-2-ylmethyl)amino]methyl}benzoic acid (15): The compound was prepared in a similar way to compound **13**. Yield: 90%. ^{1}H NMR (400 MHz, $CDCl_3$): δ = 10.00 (br, 1H), 7.89 (d, J = 8.0 Hz, 2H), 7.85 (s, 1H), 7.35 (d, J = 8.0 Hz, 2H), 7.15–7.02 (m, 4H), 6.91 (s, 1H), 6.74 (s, 1H), 5.05 (s, 2H), 3.83 (s, 2H), 3.68 (s, 2H), 3.66 (s, 2H), 3.59 (s, 3H), 3.30 (s, 3H), 2.26 ppm (s, 3H); ^{13}C NMR (100 MHz, $CDCl_3$): δ = 169.16, 147.67, 144.77, 142.76, 137.45, 136.83, 132.12, 130.75, 129.48, 129.40, 128.53, 126.41, 125.75, 124.58, 121.67, 119.62, 116.22, 95.10, 57.94, 56.16, 50.88, 49.25, 33.30, 20.33 ppm; ESI-MS: m/z: 476.2 $[M+H]^+$; HR-MS (FAB, NBA): m/z: calcd for $C_{26}H_{30}N_5O_4$: 476.2298; found: 476.2300 $[M+H]^+$.

6-{[[1-(2-Methoxymethoxy-5-methylphenyl)-1*H*-imidazol-4-ylmethyl](1-methyl-1*H*-imidazol-2-ylmethyl)amino]methyl}-*N*-{2-[10,15,20-tris(2,4,6-trimethylphenyl)porphyrin-5-yl]-phenyl}-nicotinamide (17): Triethylamine (28 μL, 0.2 mmol) and 2-chloro-1-methylpyridinium iodide (51 mg, 0.2 mmol) were added to a solution of compound **16** (76 mg, 0.1 mmol) and **13** (47 mg, 0.1 mmol) in dichloromethane. The mixture was stirred for several days under nitrogen. The progress of the reaction was monitored by TLC. After completion of the reaction, the solvent was removed and the residue was subjected to flash column chromatography (MeOH/CH_2Cl_2 8%). Yield: 76 mg, 63%. ^{1}H NMR (400 MHz, $CDCl_3$): δ = 8.87 (d, J = 8.0 Hz, 1H), 8.75 (d, J = 4.4 Hz, 2H), 8.67 (d, J = 4.4 Hz, 2H), 8.63 (d, J = 3.6 Hz, 4H), 8.03 (d, J = 7.2 Hz, 1H), 7.86 (d, J = 7.2 Hz, 1H), 7.83 (s, 1H), 7.54 (t, J = 7.2 Hz, 1H), 7.48 (s, 1H), 7.24–7.26 (m, 6H), 7.21 (s, 2H), 7.04 (s, 1H), 6.87 (s, 1H), 6.83 (s, 1H), 6.79 (d, J = 8.0 Hz, 1H), 6.63 (d, J = 8.0 Hz, 1H), 6.47 (s, 1H), 6.15 (s, 1H), 4.91 (s, 2H), 3.36 (s, 3H), 3.29 (s, 2H), 3.25 (s, 2H), 3.18 (s, 3H), 2.93 (s, 2H), 2.61 (s, 3H), 2.59 (s, 6H), 2.24 (s, 3H), 1.88 (s, 3H), 1.82 (s, 6H), 1.80 (s, 3H), 1.75 (s, 6H), −2.53 ppm (s, 2H); ESI-MS: m/z: 1214.6 $[M+H]^+$; HR-MS (FAB, NBA): m/z: calcd for $C_{78}H_{76}N_{11}O_3$: 1214.6133; found: 1214.6130 $[M+H]^+$.

6-{[[1-(2-Hydroxy-5-methylphenyl)-1*H*-imidazol-4-ylmethyl](1-methyl-1*H*-imidazol-2-ylmethyl)-amino]methyl}-*N*-{2-[10,15,20-tris(2,4,6-trimethylphenyl)porphyrin-5-yl]phenyl}nicotinamide ($L^{N4\text{-}OH}$TMP, 18): Trimethylsilyl bromide (0.13 mL, 1.0 mmol) was added to a cooled solution (−40 °C) of the above methoxymethyl ether **17** (0.12 g, 0.1 mmol) in dichloromethane (6.0 mL) containing 4 Å molecular sieves. The solution was stirred at −20 °C for 4 h and then for 4 h at 0 °C. The reaction mixture was then poured into a solution of saturated sodium bicarbonate, extracted with dichloromethane, and dried over anhydrous magnesium sulfate. The solvent was removed by evaporation and the residue was purified by flash column chromatography (MeOH/CH_2Cl_2 8%). Yield: 70 mg, 60%. ^{1}H NMR (400 MHz, $CDCl_3$): δ = 8.84 (d, J = 8.0 Hz, 1H), 8.75 (d, J = 4.8 Hz, 2H), 8.67 (d, J = 4.4 Hz, 2H), 8.63 (d, J = 3.6 Hz, 4H), 8.03 (d, J = 6.0 Hz, 1H), 7.85 (d, J = 7.2 Hz, 1H), 7.83 (s, 1H), 7.76 (s, 1H), 7.54 (t, J = 6.0 Hz, 1H), 7.24–7.26 (m, 6H), 7.20 (s, 2H), 7.14 (s, 1H), 6.82 (d, J = 8.0 Hz, 1H), 6.77 (d, J = 6.0 Hz, 1H), 6.70 (d, J = 8.0 Hz, 1H), 6.59 (d, J = 8.0 Hz, 1H,), 6.28 (s, 1H), 6.03 (s, 1H), 3.29 (s, 2H), 3.25 (s, 2H), 3.16 (s, 2H), 2.86 (s, 3H), 2.60 (s, 3H), 2.58 (s, 6H), 2.13 (s, 3H), 1.85 (s, 3H), 1.82 (s, 6H), 1.79 (s, 3H), 1.75 (s, 6H), −2.54 ppm (s, 2H); IR (KBr): $\tilde{\nu}$ = 3411, 3318, 3026, 2916, 2855, 1697, 1683, 1674, 1652, 1599, 1578, 1558, 1520, 1472, 1457, 1446, 1399, 1377, 1344, 1284, 1257, 1217, 1188, 1131, 1070, 968, 804 cm^{-1}; ESI-MS: m/z: 1170.6 $[M+H]^+$; HR-MS (FAB, NBA): m/z: calcd for $C_{76}H_{72}N_{11}O_2$: 1170.5870; found: 1170.5869 $[M+H]^+$.

[($L^{N4\text{-}OH}$)Cu^{I}-Fe^{II}(TMP)](TfO) (1a) and [($L^{N4\text{-}OMOM}$)Cu^{I}-Fe^{II}(TMP)](TfO) (1b): The preparation of [($L^{N4\text{-}OR}$)Cu^{II}-Fe^{III}(TMP)]$^+$ (**1a**: R = H, **1b**: R = MOM) has been described previously.[11]

4-{[[1-(2-Methoxymethoxy-5-methylphenyl)-1*H*-imidazol-4-ylmethyl](1-methyl-1*H*-imidazol-2-ylmethyl)amino]methyl}-*N*-{2-[10,15,20-tris(2,4,6-trimethylphenyl)porphyrin-5-yl]phenyl}-benzamide ($L^{N3\text{-}OMOM}$TMP; 19): This compound was prepared in a similar way to compound **17**. Yield: 45%. ^{1}H NMR (400 MHz, $CDCl_3$): δ = 8.94 (d, J = 8.0 Hz, 1H), 8.77 (d, J = 4.8 Hz, 2H), 8.67 (d, J = 4.8 Hz, 2H), 8.63 (d, J = 2.8 Hz, 4H), 7.97 (d, J = 7.2 Hz, 1H), 7.94 (s, 1H), 7.84 (t, J = 8.0 Hz, 1H), 7.52 (s, 1H), 7.49 (d, J = 8.0 Hz, 1H), 7.21–7.27 (m, 6H), 7.10 (d, J = 7.6 Hz, 2H), 7.04 (s, 2H), 6.89 (s, 1H), 6.79 (s, 1H), 6.60 (d, J = 8.0 Hz, 2H), 6.52 (d, J = 7.6 Hz, 2H), 4.91 (s, 2H), 3.30 (s, 2H), 3.19 (s, 2H), 3.17 (s, 3H), 3.11 (s, 2H), 2.90 (s, 3H), 2.61 (s, 3H), 2.59 (s, 6H), 2.24 (s, 3H), 1.89 (s, 3H), 1.82 (s, 6H), 1.77 (s, 9H), −2.55 ppm (s, 2H); IR (KBr): $\tilde{\nu}$ = 3419, 3322, 2921, 2855, 1717, 1676, 1610, 1578, 1559, 1516, 1457, 1446, 1384, 1345, 1304, 1248, 1157, 1139, 1081, 968, 804, 732 cm^{-1}; ESI-MS: m/z: 1213.6 $[M+H]^+$; HR-MS (FAB, NBA): m/z: calcd for $C_{79}H_{77}N_{10}O_3$: 1213.6180; found: 1213.6179 $[M+H]^+$.

[($L^{N3\text{-}OMOM}$TMP)Fe^{III}]Br (20): $FeBr_2$ (25.9 mg, 120 μmol) was added to a solution of the free base porphyrin **19** (36.4 mg, 30 μmol) in deoxygenated THF (30 mL) at reflux, and heating was continued for 3 h. After the solution had cooled to RT, an aqueous EDTA solution (0.2 M, 10 mL)

was added and the mixture was stirred for 10 min. The organic phase was separated and washed with water (3×30 mL) and with saturated NaBr solution under air and was then dried over anhydrous Na_2SO_4. The solvent was removed under vacuum and the resultant residue was purified by flash column chromatography (silica gel, MeOH/$CHCl_3$ 1:15). Yield: 35 mg, 88%. UV/Vis (THF): λ_{max} (ε) = 418 (54000), 507 (8200), 650 nm (1800 $mol^{-1}\,m^3\,cm^{-1}$); ESR (THF, 77 K): g = 5.54, 2.0; ESI-MS: m/z: 1266.5 $[M-Br]^+$; HR-MS (FAB, NBA): m/z: calcd for $C_{79}H_{74}FeN_{10}O_3$: 1266.5295; found: 1266.5326 $[M\text{-}Br]^+$.

[($L^{N3\text{-}OH}$TMP)Fe^{III}]Br (21): Trimethylsilyl bromide (0.11 mL, 0.8 mmol) was added to a cooled solution (−40 °C) of [$L^{N3\text{-}OMOM}$-Fe^{III}TMP]Br (**20**, 54 mg, 40 μmol) in dichloromethane (10.0 mL) containing 4 Å molecular sieves. The solution was stirred for 8 h at −30 °C, and the reaction mixture was then poured into a solution of saturated sodium bicarbonate (30 mL) and extracted with $CHCl_3$ (3×40 mL). The organic phase was combined, washed with saturated sodium bicarbonate and saturated NaBr solution, and dried over anhydrous Na_2SO_4. The solvent was removed by evaporation and the residue was purified by flash column chromatography (silica gel, MeOH/$CHCl_3$ 1:15). Yield: 44 mg, 80%. UV/Vis (THF): λ_{max} (ε) = 418 (62000), 504 (8200), 560 (4700), 650 nm (3300 $mol^{-1}\,m^3\,cm^{-1}$); ESR (THF, 77 K): g = 5.50, 2.0; ESI-MS: m/z: 1222.5 $[M-Br]^+$; HR-MS (FAB, NBA): m/z: calcd for $C_{77}H_{70}FeN_{10}O_2$: 1222.5033; found: 1222.5032 $[M-Br]^+$.

[($L^{N3\text{-}OH}$)Cu^{I}-Fe^{II}(TMP)](TfO) (2a): [$L^{N3\text{-}OH}$-Fe^{III}TMP]Br (**21**, 12.2 mg, 0.01 mmol) and sodium dithionite (35 mg, 0.20 mmol) were dissolved in a mixture of degassed THF (4.0 mL), toluene (6.0 mL), and water (2.0 mL). The solution was stirred at room temperature for 1 h and the color of the solution changed from brown to red. The two phases were allowed to separate and the aqueous layer was removed by pipette. The organic layer was washed with dioxygen-free water to remove inorganic salts. The solvent was evaporated under vacuum and the residue was dried for 12 h under continuous high-vacuum pumping. The deprotected compound [$L^{N3\text{-}OH}$-Fe^{II}TMP] was obtained in 94% yield (11.5 mg). UV/Vis (EtCN/CH_2Cl_2 7%): λ_{max} (ε) = 369 (18000), 436 (83000), 532 (6700), 561 nm (5600), 609 nm (2800 $mol^{-1}\,m^3\,cm^{-1}$); ESI-MS: m/z: 1223.6 $[M+H]^+$.

A degassed solution of an equimolar amount of [$Cu^{I}(CH_3CN)_4$](TfO^-) was injected into the solution of [$L^{N3\text{-}OH}$-Fe^{II}TMP] by microsyringe to give a solution of [$L^{N3\text{-}OH}Cu^{I}$-Fe^{II}TMP](TfO^-) (**2a**). The solvent was removed to dryness under reduced pressure and the solid was dried under high vacuum. A quantitative yield of (**2a**) was obtained. UV/Vis (EtCN/CH_2Cl_2 7%): λ_{max} (ε) = 428 (85000), 532 (7500 $mol^{-1}\,m^3\,cm^{-1}$); ESI-MS: m/z: 1285.3 $[M-TfO]^+$.

[($L^{N3\text{-}ONa}$)Cu^{I}-Fe^{II}(TMP)](TfO) (2b): Compound **2b** was prepared in a similar way to that described for **2a**.

[($L^{N3\text{-}ONa}$-TMP)Fe^{II}]: After reduction of compound **21** as described for **2a**, the organic phase was washed with Na_2CO_3 solution (0.1 M). The solvent was evaporated under vacuum and the residue was dried for 12 h under continuous high-vacuum pumping. The deprotonated compound [$L^{N3\text{-}ONa}$-Fe^{II}TMP] was obtained in 95% yield. UV/Vis (EtCN/CH_2Cl_2 7%): λ_{max} (ε) = 368 (16500), 437 (82000), 533 (6000), 560 nm (5500), 610 nm (2700 $mol^{-1}\,m^3\,cm^{-1}$); ESI-MS: m/z (%): 1245.6 (60) $[M+H]^+$.

[($L^{N3\text{-}ONa}$)Cu^{I}-Fe^{II}(TMP)](TfO) (2b): UV/Vis (EtCN/CH_2Cl_2 7%): λ_{max} (ε) = 428 (84000), 533 (6500 $mol^{-1}\,m^3\,cm^{-1}$). ESI-MS: m/z (%): 1307.3 (50) $[M-TfO]^+$.

[($L^{N3\text{-}OMOM}$)Cu^{I}-Fe^{II}(TMP)](TfO) (2c): MOM-protected compound **2c** was prepared by the same method as described for **2a**.

[($L^{N3\text{-}OMOM}$-TMP)Fe^{II}]: Yield 93%. UV/Vis (EtCN): λ_{max} (ε) = 426 (77000), 533 (11000), 571 nm (3700 $mol^{-1}\,m^3\,cm^{-1}$); ESI-MS: m/z (%): 1267.6 (100) $[M+H]^+$.

[($L^{N3\text{-}OMOM}$)Cu^{I}-Fe^{II}(TMP)](TfO) (2c): UV/Vis (EtCN): λ_{max} (ε) = 426 (80000), 532 (12000), 571 nm (4500 $mol^{-1}\,m^3\,cm^{-1}$); ESI-MS: m/z (%): 1329.2 (100) $[M-TfO]^+$.

Benzyl-[1-(2-methoxymethoxy-5-methylphenyl)-1*H*-imidazol-4-ylmethyl](1-methyl-1*H*-imidazol-2-yl-methyl)amine ($L^{N3\text{-}OMOM}$): This compound was prepared in a similar way to **14** with use of benzyl chloride. Yield: 43%. ^{1}H NMR (400 MHz, $CDCl_3$): δ = 7.70 (s, 1H), 7.32 (d, J = 7.2 Hz, 2H), 7.24 (t, J = 7.2 Hz, 2H), 7.17 (t, J = 7.2 Hz, 1H), 7.12 (s, 1H), 7.09 (s, 1H), 7.05 (s, 2H), 6.83 (s, 1H), 6.72 (s, 1H), 5.04 (s, 2H), 3.71 (s, 2H), 3.62 (s, 2H), 3.61 (s, 2H), 3.54 (s, 3H), 3.30 (s, 3H), 2.28 ppm (s, 3H); ^{13}C NMR (100 MHz, $CDCl_3$): δ = 147.52, 145.22, 138.80, 137.88, 136.88, 131.88, 128.84, 128.70, 127.73, 126.84, 126.48, 126.44, 125.61, 121.14, 118.87, 116.17, 94.97, 57.56, 55.91, 50.66, 49.74, 32.64, 20.19 ppm; ESI-MS: m/z: 432.2 $[M+H]^+$; HR-MS (FAB, NBA): m/z: calcd for $C_{25}H_{30}N_5O_2$: 432.2400; found: 432.2398 $[M+H]^+$.

2-(4-{[Benzyl-(1-methyl-1*H*-imidazol-2-ylmethyl)amino]methyl}imidazol-1-yl)-4-methylphenol ($L^{N3\text{-}OH}$): Cleavage of the MOM group was carried out in a similar way to that used to prepare **18**. Yield: 50%. ^{1}H NMR (400 MHz, $CDCl_3$): δ = 7.65 (s, 1H), 7.27 (d, J = 7.2 Hz, 2H), 7.22 (t, J = 7.2 Hz, 1H), 7.17 (t, J = 6.8 Hz, 2H), 7.13 (s, 1H), 6.98–6.93 (m, 3H), 6.75 (s, 1H), 6.64 (s, 1H), 3.65 (s, 2H), 3.56 (s, 4H), 3.49 (s, 3H), 2.24 ppm (s, 3H); ^{13}C NMR (100 MHz, $CDCl_3$): δ = 149.09, 145.52, 138.71, 137.09, 136.97, 129.24, 129.05, 128.64, 128.09, 126.89, 125.38, 125.26, 124.91, 121.47, 119.68, 118.04, 58.70, 51.35, 49.75, 33.17, 20.37 ppm; ESI-MS: m/z: 388.2 $[M+H]^+$; HR-MS (FAB, NBA): m/z: calcd for $C_{23}H_{26}N_5O$: 388.2137; found: 388.2130 $[M+H]^+$.

[1-(2-Methoxymethoxy-5-methylphenyl)-1*H*-imidazol-4-ylmethyl](1-methyl-1*H*-imidazol-2-ylmethyl)-pyridin-2-ylmethylamine ($L^{N4\text{-}OMOM}$): This compound was prepared in a similar way to $\mathbf{L}^{N3\text{-}OMOM}$ with use of 2-picolyl chloride hydrochloride. Yield: 41%. ^{1}H NMR (400 MHz, $CDCl_3$): δ = 8.50 (d, J = 4.8 Hz, 1H), 7.73 (s, 1H), 7.62 (t, J = 5.6 Hz, 1H), 7.47 (d, J = 8.0 Hz, 1H), 7.18 (t, J = 8.0 Hz, 1H), 7.13 (d, J = 8.0 Hz, 2H), 7.09 (s, 1H), 7.07 (s, 1H), 6.86 (s, 1H), 6.74 (s, 1H), 5.08 (s, 2H), 3.82 (s, 2H), 3.77 (s, 2H), 3.69 (s, 2H), 3.60 (s, 3H), 3.34 (s, 3H), 2.31 ppm (s, 3H); ^{13}C NMR (100 MHz, $CDCl_3$): δ = 158.86, 148.35, 147.43, 144.92, 137.35, 137.00, 135.95, 131.83, 128.84, 126.62, 126.31, 125.55, 123.03, 121.48, 121.10, 119.06, 116.07, 94.91, 59.35, 55.89, 51.05, 49.66, 32.63, 20.14 ppm; ESI-MS: m/z: 433.2 $[M+H]^+$; HR-MS (FAB, NBA): m/z: calcd for $C_{24}H_{29}N_6O_2$: 433.2352; found: 432.2352 $[M+H]^+$.

4-Methyl-2-(4-{[(1-methyl-1*H*-imidazol-2-ylmethyl)-pyridin-2-ylmethylamino]methyl}imidazol-1-yl)phenol ($L^{N4\text{-}OH}$): This compound was prepared in a similar way to $\mathbf{L}^{N3\text{-}OH}$. Yield: 45%. ^{1}H NMR (400 MHz, $CDCl_3$): δ = 8.41 (d, J = 5.2 Hz, 1H), 7.66 (s, 1H), 7.51 (t, J = 8.0 Hz, 1H), 7.39 (d, J = 8.0 Hz, 1H), 7.16 (s, 1H), 7.05 (t, J = 6.0 Hz, 1H), 6.95–6.87 (m, 3H), 6.74 (s, 1H), 6.65 (s, 1H), 3.75 (s, 2H), 3.70 (s, 2H), 3.60 (s, 2H), 3.49 (s, 3H), 2.20 ppm (s, 3H); ^{13}C NMR (100 MHz, $CDCl_3$): δ = 158.85, 148.91, 148.42, 145.23, 137.07, 136.76, 136.50, 129.20, 128.61, 125.53, 125.24, 124.70, 123.50, 121.94, 121.52, 119.74, 117.74, 61.58, 51.60, 49.80, 33.07, 20.32 ppm; ESI-MS: m/z: 389.2 $[M+H]^+$; HR-MS (FAB, NBA): m/z: calcd for $C_{22}H_{25}N_6O$: 389.2090; found: 389.2086 $[M+H]^+$.

Acknowledgements

This work was financially supported by a Grant-in-Aid for Scientific Research (S) (17105003) from the Japan Society for the Promotion of Science, as well as by grants from the Asahi Glass Foundation and the Takeda Science Foundation. J.-G.L. gratefully acknowledges the JSPS for providing a Research Fellowship for Foreign Researchers.

[1] a) S. Ferguson-Miller, G. T. Babcock, *Chem. Rev.* **1996**, *96*, 2889–2908; b) G. T. Babcock, *Proc. Natl. Acad. Sci. USA* **1999**, *96*, 12971–12973; c) T. Kitagawa, *J. Inorg. Biochem.* **2000**, *82*, 9–18; d) M. I. Verkhovsky, I. Belevich, D. A. Bloch, M. Wikström, *Biochim. Biophys. Acta* **2006**, *1757*, 401–407; e) S. Yoshikawa, K. Muramoto, K. Shinzawa-Itoh, H. Aoyama, T. Tsukihara, T. Ogura, K. Shimokata, Y. Katayama, H. Shimada, *Biochim. Biophys. Acta* **2006**, *1757*, 395–400.

[2] a) G. T. Babcock, M. Wikström, *Nature* **1992**, *356*, 301–309; b) M. Fabian, G. Palmer, *Biochemistry* **1995**, *34*, 13802–13810; c) D. A. Proshlyakov, M. A. Pressler, G. T. Babcock, *Proc. Natl. Acad. Sci. USA* **1998**, *95*, 8020–8025; d) H. Michel, J. Behr, A. Harrenga, A. Kannt, *Annu. Rev. Biophys. Biomol. Struct.* **1998**, *27*, 329–356;

e) T. L. Poulos, H. Li, C. S. Raman, *Curr. Opin. Chem. Biol.* **1999**, *3*, 131–137.

[3] a) S. Yoshikawa, K. Shinzawa-Itoh, R. Nakashima, R. Yaono, E. Yamashita, N. Inoue, M. Yao, M. J. Fei, C. P. Libeu, T. Mizushima, H. Yamaguchi, T. Tomizaki, T. Tsukihara, *Science* **1998**, *280*, 1723–1729; b) C. Ostermeier, A. Harrenga, U. Ermler, H. Michel, *Proc. Natl. Acad. Sci. USA* **1997**, *94*, 10547–10553.

[4] a) P. E. M. Siegbahn, M. R. A. Blomberg, *Biochim. Biophys. Acta* **2004**, *1655*, 45–50; b) D. A. Proshlyakov, M. A. Pressler, C. DeMaso, J. F. Leykam, D. L. DeWitt, G. T. Babcock, *Science* **2000**, *290*, 1588–1591; c) E. Pinakoulaki, U. Pfitzner, B. Ludwig, C. Varotsis, *J. Biol. Chem.* **2002**, *277*, 13563–13568; d) T. Uchida, T. Mogi, H. Nakamura, T. Kitagawa, *J. Biol. Chem.* **2004**, *279*, 53613–53620; e) J. A. Sigman, H. K. Kim, X. Zhao, J. R. Carey, Y. Lu, *Proc. Natl. Acad. Sci. USA* **2003**, *100*, 3629–3634.

[5] a) R. M. Nyquist, D. Heitbrink, C. Bolwien, R. B. Gennis, J. Heberle, *Proc. Natl. Acad. Sci. USA* **2003**, *100*, 8715–8720; b) M. M. Pereira, F. L. Sousa, M. Teixeira, R. M. Nyquist, J. Heberle, *FEBS Lett.* **2006**, *580*, 1350–1354; c) G. Capitanio, P. L. Martino, N. Capitanio, E. D. Nitto, S. Papa, *Biochemistry* **2006**, *45*, 1930–1937.

[6] a) E. Kim, E. E. Chufan, K. Kamaraj, K. D. Karlin, *Chem. Rev.* **2004**, *104*, 1077–1134; b) J. P. Collman, R. Boulatov, C. J. Sunderland, L. Fu, *Chem. Rev.* **2004**, *104*, 561–588; c) B. A. Barry, O. Einarsdottir, *J. Phys. Chem. B* **2005**, *109*, 6972–6981.

[7] a) J. P. Collman, R. A. Decreau, S. Costanzo, *Org. Lett.* **2004**, *6*, 1033–1036; b) J. P. Collman, R. A. Decreau, C. Zhang, *J. Org. Chem.* **2004**, *69*, 3546–3549.

[8] a) M. Aki, T. Ogura, Y. Naruta, T. H. Le, T. Sato, T. Kitagawa, *J. Phys. Chem. A* **2002**, *106*, 3436–3444; b) J. A. Cappuccio, I. Ayala, G. I. Elliott, I. Szundi, J. Lewis, J. P. Konopelski, B. A. Barry, O. Einarsdottir, *J. Am. Chem. Soc.* **2002**, *124*, 1750–1760; c) J. P. Collman, Z. Wang, M. Zhong, L. Zeng, *J. Chem. Soc. Perkin Trans. 1* **2000**, 1217–1221; d) K. M. McCauley, J. M. Vrtis, J. Dupont, W. A. van der Donk, *J. Am. Chem. Soc.* **2000**, *122*, 2403–2404; e) S. H. Kim, C. Aznar, M. Brynda, L. A. Silks, R. Michalczyk, C. J. Unkefer, W. H. Woodruff, R. D. Britt, *J. Am. Chem. Soc.* **2004**, *126*, 2328–2338; f) D. A. Pratt, R. P. Pesavento, W. A. van der Donk, *Org. Lett.* **2005**, *7*, 2735–2738.

[9] a) Y. Nagano, J.-G. Liu, Y. Naruta, T. Ikoma, S. Tero-Kubota, T. Kitagawa, *J. Am. Chem. Soc.* **2006**, *128*, 14560–14570; b) Y. Nagano, J.-G. Liu, Y. Naruta, T. Kitagawa, *J. Mol. Struct.* **2005**, *735*/736, 279–291; c) K. Kamaraj, E. Kim, B. Galliker, L. N. Zakharov, A. L. Rheingold, A. D. Zuberbuhler, K. D. Karlin, *J. Am. Chem. Soc.* **2003**, *125*, 6028–6029; d) R. P. Pesavento, D. A. Pratt, J. Jeffers, W. A. van der Donk, *Dalton Trans.* **2006**, 3326–3337.

[10] E. Kim, K. Kamaraji, B. Galliker, N. D. Rubie, P. Moenne-Loccoz, S. Kaderli, A. D. Zuberbuhler, K. D. Karlin, *Inorg. Chem.* **2005**, *44*, 1238–1247.

[11] J.-G. Liu, Y. Naruta, F. Tani, T. Chishiro, Y. Tachi, *Chem. Commun.* **2004**, 120–121.

[12] J.-G. Liu, Y. Naruta, F. Tani, *Angew. Chem.* **2005**, *117*, 1870–1874; *Angew. Chem. Int. Ed.* **2005**, *44*, 1836–1840.

[13] a) A. S. Hay, *J. Org. Chem.* **1962**, *27*, 3320–3321; b) M. Nakajima, I. Miyoshi, K. Kanayama, S. Hashimoto, M. Noji, K. Koga, *J. Org. Chem.* **1999**, *64*, 2264–2271.

[14] J. P. Collman, M. Zhong, *Org. Lett.* **2000**, *2*, 1233–1236.

[15] T. Chishiro, Y. Shimazaki, F. Tani, Y. Tachi, Y. Naruta, S. Karasawa, S. Hayami, Y. Maeda, *Angew. Chem.* **2003**, *115*, 2894–2897; *Angew. Chem. Int. Ed.* **2003**, *42*, 2788–2791.

[16] a) R. A. Ghiladi, K. R. Hatwell, K. D. Karlin, H.-W. Huang, P. Moenne-Loccoz, C. Krebs, B. H. Huynh, L. A. Marzilli, R. J. Cotter, S. Kaderli, A. D. Zuberbuhler, *J. Am. Chem. Soc.* **2001**, *123*, 6183–6184; b) R. A. Ghiladi, T. D. Ju, D.-H. Lee, P. Moenne-Loccoz, S. Kaderli, Y.-M. Neuhold, A. D. Zuberbuhler, A. S. Woods, R. J. Cotter, K. D. Karlin, *J. Am. Chem. Soc.* **1999**, *121*, 9885–9886; c) T. Sasaki, N. Nakamura, Y. Naruta, *Chem. Lett.* **1998**, 351–352; d) Y. Naruta, T. Sasaki, F. Tani, Y. Tachi, N. Kawato, N. Nakamura, *J. Inorg. Biochem.* **2001**, *83*, 239–246.

[17] J. P. Collman, C. J. Sunderland, K. E. Berg, M. A. Vance, E. I. Solomon, *J. Am. Chem. Soc.* **2003**, *125*, 6648–6649.

[18] E. A. Kerr, N.-T. Yu, D. E. Bartnicki, H. Mizukami, *J. Biol. Chem.* **1985**, *260*, 8360–8365.

[19] C. Varotsis, W. H. Woodruff, G. T. Babcock, *J. Biol. Chem.* **1990**, *265*, 11131–11136.

[20] a) K. Nakamoto, I. R. Paeng, T. Kuroi, T. Isobe, H. Oshio, *J. Mol. Struct.* **1988**, *189*, 293–300; b) J. P. Collman, J. I. Brauman, T. R. Halbert, K. S. Suslick, *Proc. Natl. Acad. Sci. USA* **1976**, *73*, 3333–3337; c) E. A. Kerr, H. C. Mackin, N.-T. Yu, *Biochemistry* **1983**, *22*, 4373–4379; d) M. A. Walters, T. G. Spiro, K. S. Suslick, J. P. Collman, *J. Am. Chem. Soc.* **1980**, *102*, 6857–6858.

[21] a) E. Kim, M. E. Helton, S. Lu, P. Moenne-Loccoz, C. D. Incarvito, A. L. Rheingold, S. Kaderli, A. D. Zuberbuhler, K. D. Karlin, *Inorg. Chem.* **2005**, *44*, 7014–7029; b) E. Kim, M. E. Helton, I. M. Wasser, K. D. Karlin, S. Lu, H.-W. Huang, P. Moenne-Loccoz, C. D. Incarvito, A. L. Rheingold, M. Honecker, S. Kaderli, A. D. Zuberbuhler, *Proc. Natl. Acad. Sci. USA* **2003**, *100*, 3623–3628; c) J. P. Collman, P. C. Herrmann, B. Boitrel, X. Zhang, T. A. Eberspacher, L. Fu, J. Wang, D. L. Rousseau, E. R. Williams, *J. Am. Chem. Soc.* **1994**, *116*, 9783–9784.

[22] J. E. Pate, R. W. Cruse, K. D. Karlin, E. I. Solomon, *J. Am. Chem. Soc.* **1987**, *109*, 2624–2630.

[23] a) E. E. Chufan, K. D. Karlin, *J. Am. Chem. Soc.* **2003**, *125*, 16160–16161; b) M. Selke, M. F. Sisemore, J. S. Valentine, *J. Am. Chem. Soc.* **1996**, *118*, 2008–2012; c) J. N. Burstyn, J. A. Roe, A. R. Miksztal, B. A. Shaevitz, G. Lang, J. S. Valentine, *J. Am. Chem. Soc.* **1988**, *110*, 1382–1388.

[24] a) L. M. Mirica, X. Ottenwaelder, T. D. P. Stack, *Chem. Rev.* **2004**, *104*, 1013–1046; b) E. A. Lewis, W. B. Tolman, *Chem. Rev.* **2004**, *104*, 1047–1076.

[25] a) V. S. I. Sprakel, M. C. Feiters, W. Meyer-Klaucke, M. Klopstra, J. Brinksma, B. L. Feringa, K. D. Karlin, R. J. M. Nolte, *Dalton Trans.* **2005**, 3522–3534; b) Y. Rondelez, M.-N. Rager, A. Duprat, O. Reinaud, *J. Am. Chem. Soc.* **2002**, *124*, 1334–1340.

[26] a) R. S. Blackmore, C. Greenwood, Q. H. Gibson, *J. Biol. Chem.* **1991**, *266*, 19245–19249; b) M. Oliveberg, B. G. Malmstrom, *Biochemistry* **1992**, *31*, 3560–3563; c) M. I. Verkhovsky, J. E. Morgan, M. Wikström, *Biochemistry*, **1994**, *33*, 3079–3086.

[27] R. K. Griffith, R. A. Dipietro, *Synthesis*, **1983**, 576–576.

[28] K. J. Oberhausen, J. F. Richardson, R. M. Buchanan, W. Pierce, *Polyhedron* **1989**, *8*, 659–668.

[29] G. Roelfes, M. E. Branum, L. Wang, L. Que, Jr., B. L. Feringa, *J. Am. Chem. Soc.* **2000**, *122*, 11517–11518.

[30] G. J. Kubas, *Inorg. Synth.* **1979**, *19*, 90–92.

[31] a) J. S. Linsey, R. W. Wagner, *J. Org. Chem.* **1989**, 54, 828–836; b) A. L. Balch, Y.-W. Chan, R.-J. Cheng, G. N. La Ma, L. Latos-Grazynski, M. W. Renner, *J. Am. Chem. Soc.* **1984**, *106*, 7779–7785.

Received: December 26, 2006
Published online: May 14, 2007

